Institut für Veterinärpharmakologie und –toxikologie
der Vetsuisse-Fakultät Universität Zürich
Direktor: Prof. Dr. med. vet. Hanspeter Nägeli

Arbeit unter wissenschaftlicher Betreuung von
PD Dr. med. vet. Dr. sc. nat. Enni Markkanen

The effect of persistent DNA damage on fibroblasts

Inaugural-Dissertation

zur Erlangung der Doktorwürde der
Vetsuisse-Fakultät Universität Zürich

vorgelegt von

Larissa Inglin

Tierärztin
von Sattel, SZ

genehmigt auf Antrag von

PD Dr. med. vet. Dr. sc. nat. Enni Markkanen, Referentin
Prof. Dr. med. vet. Nicole Borel, Korreferentin

2021

Table of Contents

1 Zusammenfassung

Krebszellen werden stark vom Krebs-assoziierten Stroma (CAS) beeinflusst. Eine wichtige Komponente dieses CAS sind die krebsassoziierten Fibroblasten (CAFs), welche das Tumorwachstum und die Metastasierung stark fördern. Die Basen-Exzisionsreparatur (BER) ist ein zentraler DNA-Reparaturmechanismus in Zellen, der für den Erhalt der Genomintegrität mitverantwortlich ist. Ein Knockdown (KD) des zentralen BER Proteins XRCC1 führt zu persistierenden DNA-Schäden, die eine ATF4-abhängige Stoffwechselumstellung induzieren, die die Nahrungsautarkie beispielsweise durch Autophagie erhöhen könnte. Der Zweck dieser Umprogrammierung nach XRCC1 KD ist jedoch noch unklar. In dieser Arbeit zeigen wir, dass XRCC1 KD Fibroblasten einen Überlebensvorteil unter Nährstoffmangel haben, der durch die Aktivierung der integrierten Stressreaktion mittels Signalisierung von DNA-Schäden vermittelt wird. Dies wiederum erhöht die Translation des Stress-Reaktionsfaktors ATF4. Die Autophagie wird jedoch durch XRCC1 KD nicht erhöht, was darauf hindeutet, dass der beobachtete Überlebensvorteil unabhängig von der Autophagie ist. Interessanterweise fanden wir, dass XRCC1 KD zu einer allgemeinen Abnahme des p62-Proteins durch DNA-Schadenssignalisierung mittels ATM führt. Zusammenfassend zeigen diese Ergebnisse, wie persistierende DNA-Schäden weitreichende metabolische und andere Veränderungen in Fibroblasten auslösen können, welche Relevanz für die Tumorbiologie und darüber hinaus haben.

Schlüsselwörter: Basen-Exzisionsreparatur, Krebs-assoziierte Fibroblasten, XRCC1, ATF4, Autophagie

2 Summary

Cancer is strongly influenced by the surrounding cancer-associated stroma (CAS). A prominent cellular component of CAS are the cancer-associated fibroblasts (CAFs) which strongly support tumour growth and metastasis. Base excision repair (BER) is a centrally important DNA repair mechanism in cells responsible for the maintenance of genome integrity. Knockdown (KD) of the core BER protein XRCC1 leads to persistent DNA damage, which induces ATF4-dependent metabolic rewiring that might increase nutritional self-sufficiency for example through enhancing autophagy. However, the rationale for this reprogramming following XRCC1 KD remains enigmatic. In this thesis, we show that XRCC1 KD fibroblasts have a survival advantage under nutrient starvation that is mediated through activation of the integrated stress response by DNA damage signalling, which in turn increases translation of the stress-response factor ATF4. However, autophagy is not increased by XRCC1 KD, suggesting the observed survival advantage to be independent of autophagy. Interestingly, we found that XRCC1 KD leads to a general decrease of p62 protein through DNA damage signalling by ATM. In summary, these results reveal how persistent DNA damage can trigger far-reaching metabolic and other changes in fibroblasts with relevance for tumour biology and beyond.

Keywords: Base excision repair, cancer-associated fibroblasts, XRCC1, ATF4, Autophagy

3 Abbreviations

AP site	abasic site
APE1	AP-endonuclease 1
Asn	asparagine
ASNS	asparagine synthetase
Asp	aspartate
ATF4	activating transcription factor 4
ATM	ataxia telangiectasia (A-T) mutated
BER	base excision repair
CAF	cancer-associated fibroblasts
CAS	cancer-associated stroma
CQ	chloroquine diphosphate salt
DDR	DNA damage response
eiF2α	eukaryotic translation initiation factor 2 subunit 1
FCS	foetal calf serum
GCN2	general control non-derepressible 2
H_2O_2	hydrogen peroxide
HRI	heme-regulated eIF2α kinase
ISR	integrative stress response
KD	knockdown
KO	knockout
LC3	microtubule-associated protein 1A/1B-light chain 3
Lig IIIα	DNA ligase III α
p62/SQSTM1	sequestosome-1
PC	pyruvate carboxylase
PKR	double-stranded RNA-dependent protein kinase
PERK	protein kinase RNA-like endoplasmic reticulum kinase
Pol β	DNA polymerase β
ROS	reactive oxygen species
RT-qPCR	quantitative real-time PCR
SSB	DNA single strand break
TCA	tricarboxylic acid
TGF β	transforming growth factor β
XRCC1	X-ray repair cross complementing 1

4 Introduction

4.1 Cancer and cancer-associated stroma

"Cancer" is a term that stands for a large group of diseases that can occur anywhere in the body. A similarity shared by all different forms of cancer is that the tumour cells are fast growing, abnormal cells which are often able to invade the surrounding tissue and metastasise to distant body parts [1]. By doing so, cancer cells compromise the function of single organs and sometimes even the entire body, which can ultimately lead to death. Indeed, cancer is the second leading cause of death worldwide; in numbers that translates to about 10 million people that died because of cancer in 2020 [2]. Considering this, further research is really important to better understand the mechanisms behind cancer biology that allows to improve treatments for affected patients.
Until quite recently, cancer research focused entirely on the abnormally growing tumour cells themselves, without paying much attention to the surrounding tissue. However, more recently, scientists have started to appreciate the importance of the non-cancerous tissue that surrounds cancer cells, termed CAS, that strongly influences cancer growth and metastasis [3,4]. CAS is defined as the non-malignant cells and their stroma that is found within and next to the tumours [3,5]. Among other constituents such as immune cells, angiogenetic vascular cells and extracellular matrix, fibroblasts are an important component of CAS. Unlike normal fibroblasts, these CAFs show an activated phenotype similar to what is found during wound healing. Importantly, these CAFs are not just quiescent cells, but instead they are able to strongly support tumour growth, inflammation, angiogenesis and metastasis through a wide variety of mechanisms [3,6,7]. Hence, cancer cells do not manifest the disease alone, but strongly depend on the normal surrounding cells, which constitute a major factor for tumour outcome [8]. Considering the importance of the CAS and especially CAFs for growth and metastasis of tumours, targeting these components is viewed as a promising method for the development of novel therapeutic options to treat cancer [7]. Such CAF-focused therapies are thought to optimally complement the existing mostly tumour-cell targeting therapeutic approaches. However, the current knowledge regarding CAFs biology is still far from complete and warrants further investigation.

4.2 DNA base-excision repair

Mutations in the DNA are the molecular trigger for the development of most cancers. Such DNA mutations are usually caused by DNA damage. DNA damage can arise from different exogenous or endogenous sources. Examples for exogenous sources of DNA damage include exposure to ionizing radiation, UV light, or harmful chemicals, to name a few. But DNA damage can also arise even in the absence of exogenous DNA damaging agents, because the chemical reactivity of DNA in the aquatic milieu renders it prone to spontaneous alterations. The combined actions of such endogenous and exogenous DNA damaging agents lead to a high level of DNA damage that is constantly present in the cells of our body. This also means that, to avoid deleterious mutagenic and cytotoxic consequences of DNA damage, the cells need intricate mechanisms to repair such DNA lesions in order to maintain their genome integrity [9-11]. One of these mechanisms is BER. BER is responsible for correcting DNA single strand breaks (SSBs) and small base lesions, which are frequently occurring DNA lesions [11,12]. BER is a well-studied process that allows the recognition and removal of corrupted bases, and correct sealing of single-strand breaks. BER can roughly be divided into three steps: i) damage-specific DNA glycosylases scan the DNA, recognise corrupted bases, and catalyse the excision of such damaged bases, leaving a 'gap' in the DNA. ii) These 'gaps' are further processed by the AP-endonuclease 1 (APE1). APE1 cleaves the DNA sugar-phosphate backbone at 5' to the AP site, thereby generating a SSB, and trims the DNA ends so they are chemically compatible with the next step. iii) Finally, a protein complex consisting of DNA polymerase β (Pol β), DNA ligase IIIa (Lig III) and XRCC1 is recruited to fill the gap by adding missing nucleotides and to seal the DNA ends to create a fully double-stranded DNA

again [11,12]. Of note, the protein XRCC1 that is involved in this final step does not have any enzymatic activity. Rather, XRCC1 acts as scaffold protein that plays a key role in stabilising the Pol β and Lig III complex. Thus, in the absence of XRCC1, the levels of Pol β and Lig III are dramatically reduced, which leads to cells that display a deficiency in DNA repair and increased genomic instability [12-14]. To ensure maintenance of genetic integrity, levels of BER proteins have been shown to be tightly adapted to cellular needs – when there is much DNA damage, levels of BER components are increased, and when the damage is repaired again, the levels are lowered again to baseline [15-18]. Accordingly, there is a plethora of reports showing deregulation of XRCC1 levels in different types of cancer (reviewed in [11]). Furthermore, a knockout (KO) of XRCC1 in the whole mouse is embryonically lethal, presumably through accumulation of unrepaired DNA damage, which is not compatible with physiological development [19,20]. A brain-specific KO of XRCC1 in mice (driven by Nestin-Cre) shows age-dependent accumulation of DNA damage, loss of cerebellar interneurons and altered hippocampal homeostasis [21]. Finally, biallelic mutation in XRCC1 in humans are associated with progressive cerebellar ataxia, ocular motor apraxia and peripheral axonal neuropathy [22].
In summary, BER is a highly important protection shield to safeguard cellular DNA against frequently occurring DNA lesions, and XRCC1 is a key molecule to ensure the proper function of BER.

4.3 A connection between cancer-associated fibroblasts and the base-excision repair

When it comes to understanding CAF biology, one of the key questions is to elucidate the molecular triggers that cause activation of normal fibroblasts into CAFs. If we understand how CAFs are activated, this could potentially lead to the development of approaches to hinder this activation and thereby curb their tumour-supportive function. So far, it has been shown that inflammatory cytokines, such as transforming growth factor β (TGF β) and/or reactive oxygen species (ROS) can activate normal fibroblasts and transform them into CAFs [23,24]. However, the exact molecular mechanism behind these observations remained obscure. Of note, when cells are exposed to ROS, one of the most important effects is the generation of oxidative DNA damage [10,11]. This suggests a possible role for oxidative DNA damage in activation of CAFs. Consistent with this, persistent DNA damage, induced through a downregulation of XRCC1 by siRNA in human primary fibroblasts, has been shown to induce gene-expression changes that are comparable to those found in tumours [13]. Furthermore, exposure of normal fibroblasts to the pro-inflammatory cytokine TGF β or ROS for an extended period was found to induce a BER deficiency through downregulation of XRCC1, suggesting a potential role for decreased BER in the activation of CAFs [25]. Accordingly, a downregulation of XRCC1 in fibroblasts led to a decreased BER capacity and persistent DNA damage, that in turn induced normal fibroblasts to transform into a CAF-like phenotype capable of supporting growth and motility of cancer cells *in vitro*. It was shown that the stress-responsive transcription factor ATF4 was at least partially accountable for this reprogramming [13,25]. Taken together, prolonged exposure to pro-inflammatory cytokines and ROS can induce a deficiency in BER through transcriptional down-regulation of XRCC1, which in turn leads to the transformation of normal fibroblasts into cancer-cell supporting CAFs.
Given the literature about adaptation of BER enzyme levels to the status of DNA damage in cells to ensure timely repair of these lesions [15-18], the observation that prolonged exposure of fibroblasts to persistent DNA damaging agents led to a decrease in BER capacity was somewhat counterintuitive. This sparked the question, why these cells would opt to down-regulate XRCC1 under stressful circumstances, instead of increasing their BER capacity to be able to combat DNA damage. The Markkanen group has previously shown that knockdown of XRCC1 in primary fibroblasts causes a wide-ranging reprogramming of the cellular metabolism including anabolic changes [13]. Further analysis showed vast adjustments that cause cellular metabolism to shift away from the use of the tricarboxylic acid (TCA) cycle and towards the use of the one-carbon cycle or the pentose phosphate pathway [Legrand et al, unpublished observations]. Such changes could

benefit the cells by bringing about a self-sufficiency that renders them independent of many exogenous metabolites, such as amino acids, nucleotides and energy. ATF4 was found to be relevant for these metabolic changes. ATF4 is a transcription factor that is known as the main effector of the integrated stress response (ISR). In this context, during stressful conditions, ATF4 facilitates the expression of several genes involved in anabolic metabolism [26]. In summary, there is evidence suggesting a connection between downregulated BER capacity and a rewiring of the cellular metabolism, but the consequences of this connection remain unclear.

4.4 Autophagy and cancer-associated fibroblasts

Autophagy is a mechanism relevant for maintaining cellular homeostasis by degrading intracellular compounds inside lysosomes [27]. It can be activated in response to a variety of stressful conditions, such as nutrient starvation, damaged organelles and ER stress [28]. Autophagy enables the cell to maintain its energy status despite a shortage of exogenous nutrients, because degradation products can be released from lysosomes and re-used again [29,30]. Autophagy usually is categorized into three groups, namely macroautophagy, microautophagy and chaperon-mediated autophagy (CMA). Of these, macroautophagy (hereinafter autophagy) is the form that is characterised best [28,31]. In general, the procedure of macroautophagy requires the intracellular formation of a double-membrane organelle, the so-called autophagosome, that then fuses with the lysosome. The contents of the arising autolysosome are then degraded by lysosomal enzymes [31,32]. There is evidence suggesting that ATF4 is involved in the regulation of autophagy by inducing the transcription of the essential autophagy gene Map1lc3b [30,33].
In addition to playing a role in the response of cells to ‘canonical stress’, autophagy was found to be relevant for the ‘reverse Warburg effect’. The reverse Warburg effect describes a model where cancer cells and CAFs are viewed as two metabolically coupled compartments. Cancer cells are thought to induce oxidative stress in the adjacent stroma by secreting hydrogen peroxide what leads to mitochondrial dysfunction in CAFs. As a reaction to this, autophagy, mitophagy and aerobic glycolysis are activated in CAFs, which then produce nutrients that in turn can feed cancer cells [34-37]. Hence, autophagy might have an important role in providing CAF-generated nutrients for cancer cell growth.
The monitoring of autophagy can be performed using two different approaches: either by observation of structures that are directly related to autophagy or the quantification of proteins and organelles that are degraded during the process. In both cases, estimation of autophagic activity by determining the autophagic flux instead of analysing autophagy-related structures at a certain static timepoint is considered to be more accurate [31,32].
The most prominent marker to monitor autophagic activity is microtubule-associated protein 1 light chain 3 (LC3). Immediately after translation LC3 is processed into LC3-I. During autophagy, LC3-I is conjugated to phosphatidylethanolamine (PE) to form LC3-II, which is then recruited to autophagosomal membranes. Finally, when the autophagosome fuses with the lysosome, LC3-II gets degraded [38]. Thus, the conversion of LC3-I to LC3-II reflects the progression of autophagy and the amount of LC3-II the number of autophagosomes present at a given time point. But it is important to consider, that in the following step of degradation, LC3-II gets degraded. Hence, inhibition of autophagosome degradation causes an accumulation of LC3-II. In addition, LC3-II sometimes can be ectopically found on non-autophagic structures. So absolute LC3-II amount does not stand for autophagic activity [31,32,39]. Instead, it is better to assess the autophagic flux, that means measuring lysosome-dependent degradation of LC3-II during a certain time period. This is done by measuring LC3-II protein levels of cells treated with an autophagy inhibitor for a defined period of time compared to the level in untreated cells [31].
Another popular marker to investigate autophagy is observing the degradation of p62, also known as sequestosome 1 (SQSTM1) in humans. p62 is a scaffold protein with various functions in other processes besides autophagy, for example apoptosis, inflammation, cell survival and tumorigen-

esis [40]. p62 binds directly to LC3, which is thought to be relevant for delivering selective autophagic cargo for degradation by autophagy. Furthermore, p62 is itself degraded by the autophagy process [31,32]. Because of this selective degradation, p62 protein levels decrease when autophagy is active and, on the contrary, p62 accumulates when autophagy is inhibited [41]. Levels of both of these markers - LC3 and p62 - can be monitored by Western blotting. According to literature, autophagy could play an important role in response to several stressful conditions such as nutrient starvation, damaged organelles and ER stress [28].
Concluding, autophagy is important to promote cell survival under stressful conditions, including nutrient starvation. Furthermore, autophagy has also been implicated in CAFs, and its activity is best monitored using the two markers LC3 and p62.

4.5 Roles of p62 apart from autophagy

p62 is a multidomain protein best known for its role in autophagy, where it acts as an adapter protein. But recent research has unveiled that, apart from autophagy, it is also involved in multiple other cellular functions such as apoptosis, inflammation, metabolic reprogramming, cell survival, cell death, signal transduction and tumorigenesis where it interacts with several key components as signalling hub [40,42-44]. Out of these, particularly the connection to metabolic reprogramming and cell survival is interesting in view of this project. p62 was found to be downregulated in CAS of many tumours, and a downregulation of p62 was able to induce transformation of normal fibroblasts into CAFs able to support tumour growth [42,45,46]. In addition, this downregulation of p62 in CAFs was found to promote cell survival under nutrient restricted conditions through an upregulation of ATF4 [47]. ATF4 was found to be polyubiquitinated through a p62 dependent mechanism. When p62 expression is lost, this polyubiquitination of ATF4 is impaired, which leads to higher stability and accumulation of ATF4 protein [47,48]. This in turn enhances pyruvate carboxylase (PC) expression and upregulates asparagine synthetase (ASNS), which is known as a direct transcriptional target of ATF4 [49]. Altogether this leads to metabolic changes that enhance glucose flux into the TCA cycle and the production of non-essential amino acids, such as aspartate (Asp) and asparagine (Asn) [47]. These changes were found to be relevant under glutamine-deprived conditions, which is interesting since glutamine is often found to be depleted in solid tumours [50-52].
Taken together p62 is an interesting target involved in CAF biology, that seems to share some similarities with XRCC1: deficiency of both can lead to the activation of CAFs and seems to provoke metabolic changes that facilitate the survival of these cells under stressed conditions. It is however not known whether there exists a connection between XRCC1 and p62.

4.6 Aim of this thesis

Resent research has started to unveil a central role of CAFs in the biology of cancer development and progression. Nevertheless, the exact mechanism that lies behind CAF formation and the effects of CAFs on cancer cells are not thoroughly understood. We recently showed that prolonged exposure to pro-inflammatory cytokines or the downregulation of XRCC1 by siRNA in fibroblasts causes the accumulation of persistent DNA damage that leads to the transformation of normal fibroblasts into CAFs. ATF4 was found to be relevant for this reprogramming and it seemed to shift the cellular metabolism towards nutritional self-sufficiency. However, the reason for and consequences of this metabolic shift remained unclear.
Based on this, we formulated the following hypothesis: Could it be that the downregulation of BER capacity in fibroblasts upon exposure to a pro-inflammatory CAF-triggering environment helps cells to re-wire of their metabolism in a way that allows these cells to become more independent of available nutrients?
Hence, the aim of this work was to i) understand whether downregulation of XRCC1 could enhance cellular survival under nutrient restriction, and if so, ii) to investigate whether activation of autophagy could be a driving force behind such a survival advantage.

5 Material and Methods

In the following, only the material and methods for the second, unpublished part of this thesis are listed. The respective information to accompany the published paper can be found therein (see chapter 6.1).

5.1 Cell culture

TIG-1 primary human fibroblasts were purchased from Coriell. They were cultured under standard conditions (37 °C, 5% CO2) in Gibco™ DMEM, low glucose, GlutaMAX™ Supplement, pyruvate containing 15% foetal calf serum (FCS) if not indicated otherwise. For the experiments cells between passage 14 to 20 were used.

5.1.1 siRNA transfection

One million TIG-1 cells were seeded in 10 cm diameter petri dishes the day before transfection. Lipofectamine™ RNAiMAX Transfection Reagent (Invitrogen) was used for siRNA delivery according to manufacturer's protocol. siRNAs were purchased from Eurogentec or Thermo Fisher, sequences are specified in Table 1.
An unspecific, nontargeting sequence was used as control to mimic the procedure of transfection and to achieve an appropriate level of KD for ATF4 two siRNA sequences were used in combination. As ASNS was targeted the first time in this research, two independent siRNA sequences were used to exclude off-target effects.

siRNA	Sequence	Manufacturer	Reference/ cat. number
siControl	Manufacturer's proprietary information	Eurogentec	SR-CL000-005
siXRCC1-1	5'-AGGGAAGAGGAAGUUGGAU-3'	Eurogentec	[53]
siXRCC1-3	5'-GCUUGAGUUUUGUACGGUU-3'	Eurogentec	[13]
siATF4-1	5'-GCCUAGGUCUCUUAGAUGA-3'	Eurogentec	[13]
siATF4-2	5'-CUGCUUACGUUGCCAUGAU-3'	Eurogentec	[13]
siPERK	5'-GUGACGAAAUGGAACAAGA-3'	ThermoFisher	Assay ID s18102
siASNS-1	5-GGGUAGAGAUACAUAUGGA-3	Eurogentec	[54]
siASNS-2	5-UAUGUUGGAUGGUGUGUUU-3′	Eurogentec	[54]

Table 1: siRNA used for transfection.

5.1.2 Analysis of autophagic flux

To assess the autophagic flux in control and XRCC1 KD cells chloroquine diphosphate salt (CQ, SigmaAldrich, cat. no. C6628) was used as an inhibitor of autophagy. CQ was dissolved in dH_2O at a concentration of 20 mM as a stock solution.
For the assay two dishes with one million TIG-1 cells were seeded, the next day transfection with siCon and siXRCC1 was performed and on day three the cells were split to two new dishes. On day four the inhibitor treatment was done by removing the media, washing once with filtered PBS and adding new medium containing chloroquine at a concentration of 20 μM. Control dishes were treated with the same amount of dH_2O. After two hours of incubation the cells were collected by scraping them of the petri dish in cold PBS.

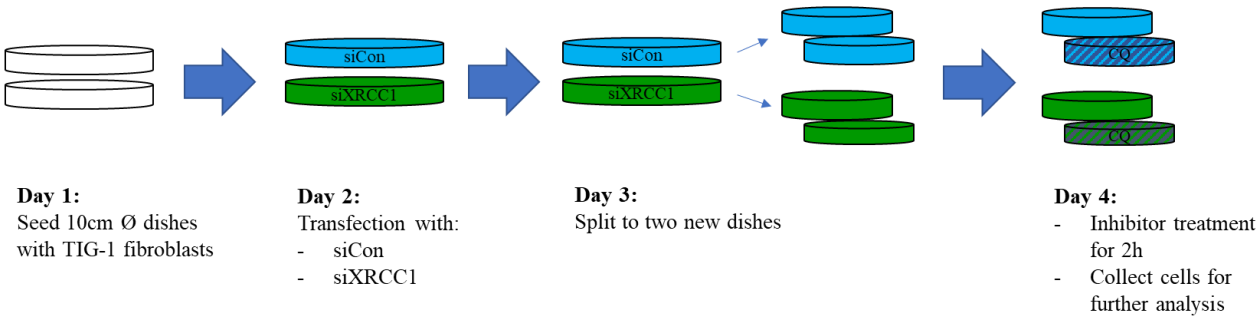

Figure 1: Scheme of experimental setup to investigate the autophagic flux in XRCC1 KD and control cells.

5.1.3 Inhibitor treatment for protein analysis

For inhibitor treatment ATMi Ku-60019 (ATMi, SigmaAldrich) was dissolved in DMSO at a concentration of 10 mM as a stock solution and used at a final concentration of 10 µM.
One million TIG-1 cells were seeded day before transfection. Every 24 h the medium was changed and fresh inhibitor or equivalent amount of DMSO was added. The treatment was started one hour after transfection for a total of three days.

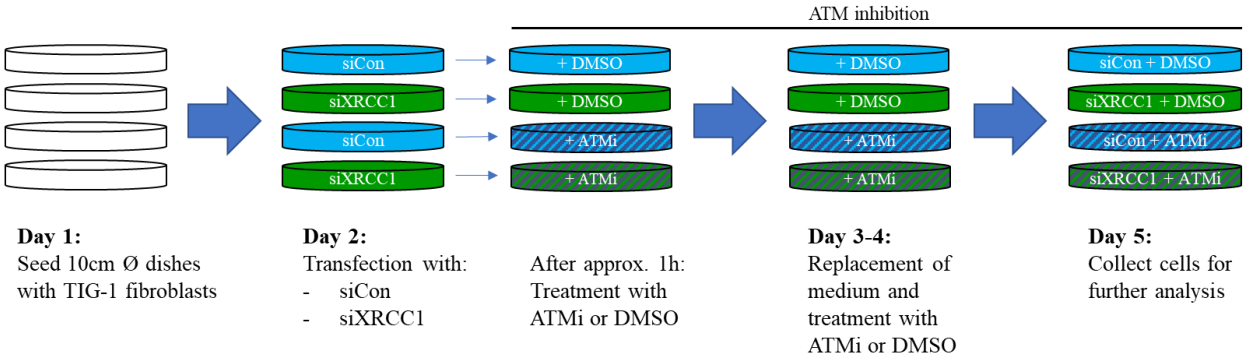

Figure 2: Scheme of experimental setup to investigate the effect of ATM inhibition on selected protein levels.

5.1.4 siRNA KD for protein analysis

Four 10 cm dishes with one million cells were seeded. The next day, two dishes were transfected with siCon and siXRCC1, the third dish with either pooled siATF4-1 and -2 or siPERK and the fourth with a combination of siXRCC1 with siATF4-1 and -2 or siPERK. Three days after transfection, the cells were scraped of the petri dishes in cold PBS to collect them for further analysis.

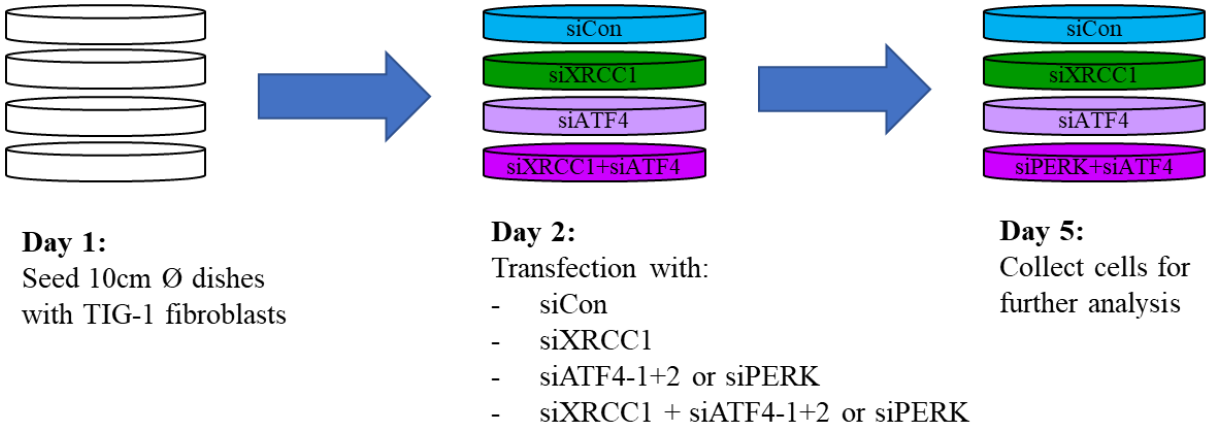

Figure 3: Scheme of experimental setup to investigate the effect of specific KDs on selected protein levels.

5.1.5 H_2O_2 treatment

For this experiment three 10 cm dishes with TIG-1 fibroblasts were seeded. One of the dishes containing 600'000 and the other two containing one million cells. The dishes containing more cells were treated with either 25 µM or 50 µM H_2O_2 for the following three days, the other dish was used as control. The medium was changed every time with the treatment.

5.1.6 Cell survival assay

On day one six 10 cm dishes were seeded in standard medium containing 15% FCS. The day after, transfection with siCon, siXRCC1, siASNS-1, siASNS-2 and a combination of siXRCC1 with each of the siASNS sequences was done. On the third day the dishes were split to two new dishes and to one dish DMEM with low amount of FCS was added, the other one was cultured under normal FCS condition. Three days after transfection, pictures of the living cells were taken with EVOS® FL Auto Microscope. Right afterwards the cells were collected for further analysis by scraping them of the dish in cold PBS.

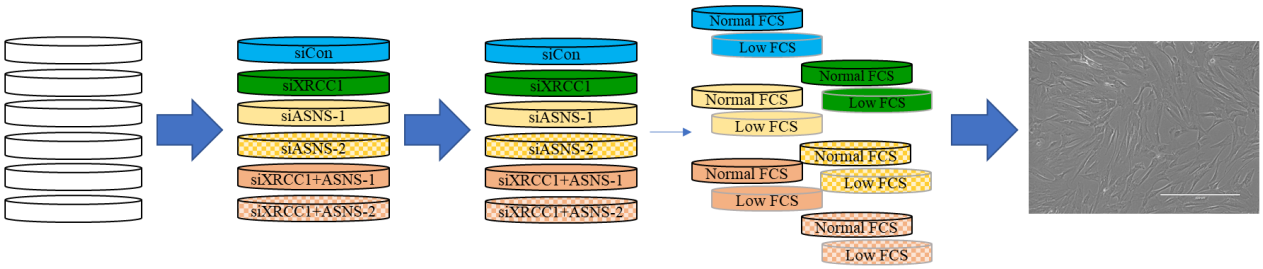

Day 1:
Seed 10cm Ø dishes with TIG-1 fibroblasts

Day 2:
Transfection with:
- siCon
- siXRCC1
- siASNS-1
- siASNS-2
- siXRCC1 + siASNS-1
- siXRCC1 + siASNS-2

Day 3:
Split to DMEM containing different concentration of FCS

Day 5:
- Cell pictures
- Collect cells for further analysis

Figure 4: Scheme of experimental setup to investigate the survival advantage of TIG-1 fibroblasts with specific KDs under nutrient restricted conditions.

5.2 mRNA isolation and RT-qPCR

5.2.1 Extraction and quantification of mRNA

RNeasy® Mini Kit by QIAGEN was used according to manufacturer's protocol "Purification of Total RNA from Animal Cells using Spin Technology" to extract mRNA.
mRNA quality and yield were measured with Thermo Scientific™ NanoDrop™ 2000/2000c Spectrophotometer according to the manufacturer's protocol.

5.2.2 Reverse transcription

For reverse transcription 1000 ng of RNA was diluted in dH_2O and reverse transcribed with Bio-Rad iScript™ cDNA Synthesis Kit according to the manufacturer's protocol using the LabCycler (SensoQuest). Then the cDNA was diluted 1:5 in dH_2O and stored at -80°C until further analysis.

5.2.3 RT-qPCR

Quantitative real-time PCR (RT-qPCR) was performed using the KAPA SYBR® FAST One-Step RT-qPCR Kit. The samples were run in duplicates, each in a total volume of 10 µl containing 2 µl of sample, on the CFX384 Touch™ Real-Time PCR detection system (Bio-Rad). Primers are detailed in the following Table 2.
Relative gene expression was quantified using the comparative CT method, normalising the values to the housekeeping genes B2M and GAPDH and to the control. The results were expressed as fold change in mRNA levels over control cells.

Gene target	Sequence	Reference
XRCC1	Fw: 5'-AACACGGACAGTGAGGAACA-3' Rw: 5'-GCTGTGACGTATCGGATGAG-3'	[13]
ATF4	Fw: 5'-GGGACAGATTGGATGTTGGAGA -3' Rw: 5'-ACCCAACAGGGCATCCAAGT-3'	[13]
ASNS	Fw: 5'-CTGCACGCCCTCTATGACA-3' Rw: 5'-TAAAAGGCAGCCAATCCTTCT-3'	[55]
P62/ SQSTM1	Fw: 5'-TGCCCAGACTACGACTTGTG-3' Rw: 5'-AGTGTCCGTGTTTCACCTTCC-3'	[56]
B2M	Fw: 5'-ATGTCTCGCTCCGTGGCCTTA-3' Rw: 5'-ATCTTGGGCTGTGACAAAGTC -3'	[25]
GAPDH	Fw: 5'-AGCCACATCGCTCAGACAC-3' Rw: 5'-GCCCAATACGACCAAATCC-3'	[13]

Table 2: List of primers used for RT-qPCR

5.3 Western blot

5.3.1 Protein extraction

Whole cell extracts from collected TIG-1 cells were prepared by adding M-PER™ Mammalian Protein Extraction Reagent supplemented with the cOmplete™, Mini, EDTA-free Protease Inhibitor Cocktail (Roche) as lysis buffer to the Eppendorf® Tubes containing the cell pellet. The tubes were then kept on a rotator wheel for 30 minutes. This was followed by three cycles of sonication with Bioruptor® plus, each cycle consisting of 30 sonication followed by 30 seconds pause. To separate the protein, the lysate was centrifuged for 20 minutes at 16050 rcf and the supernatant was transferred to a new 1.5 ml the Eppendorf® Safe-Lock tube and stored in -80 °C. The whole procedure was performed at +4 °C.

5.3.2 Total protein quantification

The Bradford assay was used according to manufacturer's protocol. Each sample was measured in double and BSA standard solution at a known concentration was used to calculate the amount of total protein in each sample.

5.3.3 Gel preparation

Depending on the experiment 20 to 40 µg of total protein were loaded with the corresponding amount of 4x leammli loading buffer. The samples were boiled at 95 °C for 5 minutes and then loaded to Criterion™ TGX Stain-Free™ Precast Gels 4-20% (BioRad). The gel was run with PowerPac™ HV (BioRad) at 150 V for 1 hour.

5.3.4 Western blotting

The separated proteins were transferred onto Trans-Blot® Turbo™ Midi 0.2 µm Nitrocellulose membrane (BioRad) using the Trans-Blot® Turbo™ Transfer System (BioRad) with settings for mixed molecular weight proteins. After transfer the membrane was blocked with 1:1 Odyssey® Blocking Buffer (PBS) in PBS for 1 h at room temperature.

5.3.5 Antibodies and analysis

After incubation with primary antibody, the membrane was washed three times with PBS containing 0.1% tween and then the corresponding secondary antibody conjugated with Alexa Fluor 680 or IRDye 800CW (both Li-cor Biosciences) was added.
Both primary and secondary antibodies were prepared in 1:1 Odyssey® Blocking Buffer (PBS) and PBST.
For detection of the signal the membrane was scanned with Odyssey® CLx and Image StudioTM was used for visualisation and to quantify the protein bands.

Antibody	**Manufacturer, order no.**	**Isotype**
ATM	Cell Signaling, #2873	Rabbit monoclonal
PERK	Cell Signaling, #3192	Rabbit monoclonal
p62/ SQSTM1	Cell Signaling, #5114S	Rabbit polyclonal
LC3A/B	Cell Signaling, #4108S	Rabbit polyclonal
Actin	SigmaAldrich, MAB1501R	Mouse monoclonal

5.4 Statistical analysis and graphical display of results

All statistical analysis and graphic display were performed with the program GraphPad Prism (www.graphpad.com). One-way ANOVA was used, followed by Bonferroni's Multiple Comparison Test to assess significance between the groups. A statistical significance level of $p < 0.05$ was applied.

6 Results

6.1 Paper: “Persistent DNA damage triggers activation of the integrated stress response to promote cell survival under nutrient restriction”

BMC Biol. (2020) 18:36 doi: 10.1186/s12915-020-00771-x.

In this paper, we show a previously unappreciated connection between persistent DNA damage and the integrated stress response (ISR). Here, chronic DNA damage, which is triggered by a decrease in BER capacity or direct exposure to DNA damaging agents, causes a strong metabolic reprogramming towards cellular self-sufficiency that promotes cell survival under nutrient restriction.
My contribution to this paper, of which I am second author, was to show that XRCC1 KD TIG-1 fibroblasts survive better than control cells under serum restriction (Figure 1 A-E). In addition, I identified a first hint for a connection to the ISR, because the survival advantage of cells upon XRCC1 KD could be rescued completely with a co-KD of ATF4 and XRCC1 (Figure 2 A-E). And I also showed that an increase of ATF4 could be observed in both, mRNA and protein levels (Figure 2F and Figure 3A).

Clementi et al. BMC Biology (2020) 18:36
https://doi.org/10.1186/s12915-020-00771-x

BMC Biology

RESEARCH ARTICLE Open Access

Persistent DNA damage triggers activation of the integrated stress response to promote cell survival under nutrient restriction

Elena Clementi, Larissa Inglin, Erin Beebe, Corina Gsell, Zuzana Garajova and Enni Markkanen*

Abstract

Background: Base-excision repair (BER) is a central DNA repair mechanism responsible for the maintenance of genome integrity. Accordingly, BER defects have been implicated in cancer, presumably by precipitating cellular transformation through an increase in the occurrence of mutations. Hence, tight adaptation of BER capacity is essential for DNA stability. However, counterintuitive to this, prolonged exposure of cells to pro-inflammatory molecules or DNA-damaging agents causes a BER deficiency by downregulating the central scaffold protein XRCC1. The rationale for this XRCC1 downregulation in response to persistent DNA damage remains enigmatic. Based on our previous findings that XRCC1 downregulation causes wide-ranging anabolic changes, we hypothesised that BER depletion could enhance cellular survival under stress, such as nutrient restriction.

Results: Here, we demonstrate that persistent single-strand breaks (SSBs) caused by XRCC1 downregulation trigger the integrated stress response (ISR) to promote cellular survival under nutrient-restricted conditions. ISR activation depends on DNA damage signalling via ATM, which triggers PERK-mediated eIF2α phosphorylation, increasing translation of the stress-response factor ATF4. Furthermore, we demonstrate that SSBs, induced either through depletion of the transcription factor Sp1, responsible for XRCC1 levels, or through prolonged oxidative stress, trigger ISR-mediated cell survival under nutrient restriction as well. Finally, the ISR pathway can also be initiated by persistent DNA double-strand breaks.

Conclusions: Our results uncover a previously unappreciated connection between persistent DNA damage, caused by a decrease in BER capacity or direct induction of DNA damage, and the ISR pathway that supports cell survival in response to genotoxic stress with implications for tumour biology and beyond.

Keywords: DNA repair, DNA base-excision repair, DNA base damage, DNA single-strand breaks, DNA double-strand breaks, DNA damage response, Integrated stress response, Tumour microenvironment, Tumour stroma

* Correspondence: enni.markkanen@vetpharm.uzh.ch
Institute of Veterinary Pharmacology and Toxicology, Vetsuisse Faculty, University of Zürich, 8057 Zürich, Switzerland

Background

DNA damage is considered the molecular origin of many pathophysiological processes such as ageing, neurodevelopmental and neurodegenerative disorders, and cancer [1–3]. Sources of DNA damage include a wide variety of exogenous damaging agents. However, even in the absence of exogenous noxious influences, DNA is prone to spontaneous alterations, due to its chemical reactivity in the aquatic milieu and reactive side-products that are created by the cellular metabolism [4]. This leads to a high level of DNA lesions even under physiological 'unstressed' circumstances that are in constant need of repair to avert potential mutagenic and cytotoxic consequences [5]. Base-excision repair (BER) is a centrally important DNA repair mechanism responsible for correcting many of these small base lesions and single-strand breaks [6]. BER is a highly coordinated process in which the scaffold protein XRCC1 occupies a critical role due to its ability to stabilise the two other core BER components DNA polymerase β and DNA ligase III [7, 8]. Therefore, depletion of XRCC1 leads to loss of the core BER machinery, and cells deficient in XRCC1 display reduced DNA repair which causes an accumulation of persistent DNA damage and an increase in genomic instability [6, 9]. DNA repair deficiencies have been strongly implicated in the development of cancer, due to increased mutation rate, interference with transcription, or generation of toxic double-strand breaks (DSBs), all of which can lead to cellular transformation [10–14]. Likewise, haploinsufficiency in XRCC1 enhances formation of precancerous lesions [15], and selective depletion of neural XRCC1 or Ape1, another BER component, leads to the development of brain tumours in mice [16, 17]. Moreover, expression of XRCC1 has been shown to be decreased in various different tumours, with lower XRCC1 levels associated with higher proliferation and shorter overall survival [18–23]. Hence, to avoid deleterious consequences of mutations and maintain DNA integrity, the capacity for DNA repair has to be tightly adapted to cellular needs [24, 25].

Recently, we have demonstrated that prolonged exposure to the pro-inflammatory cytokine TGFβ or reactive oxygen species (ROS) causes a deficiency in BER by decreasing XRCC1 expression in human primary fibroblasts [26]. This decrease in XRCC1 levels resulted in a lowered BER capacity and led to accumulation of persistent DNA damage. Mechanistically, persistent DNA damage was found to induce ATM-dependent degradation of the transcription factor Sp1, which controls XRCC1 expression, therefore creating a BER deficiency through decreasing transcription of XRCC1 [27]. Thus, somewhat counterintuitive to what would be expected for maintenance of DNA integrity in response to stressful conditions, cellular BER capacity is curbed through downregulation of XRCC1 in response to persistent DNA damage. The rationale for this reduction of BER capacity in response to persistent DNA damage remains enigmatic.

We have previously shown that a BER deficiency, brought about by downregulation of XRCC1 by siRNA, induces wide-ranging gene-expression changes in cellular metabolism that are comparable to changes found in tumours [28]. This reprogramming of cellular metabolism led to anabolic changes upon BER deficiency and was found to be at least partially dependent on the stress-responsive transcription factor ATF4 [26, 28]. As key component of the integrated stress response (ISR), ATF4 is a transcription factor that induces metabolic adaptations to stressful conditions to ensure survival [29]. As such, ATF4 mounts appropriate responses in response to a variety of different stresses, including nutrient deprivation, hypoxia, viral infections, and endoplasmic reticulum stress, and it has been shown to have important roles in cancer [30, 31]. Activation of the ATF4 and ISR in response to these stressors is mediated through activation of one of the stress-responsive eIF2α kinases GCN2, PERK, HRI, or PKR, which in turn phosphorylate eIF2α. While phosphorylation of eIF2α leads to a global repression of translation, it selectively increases the translation of ATF4 due to alternate use of open reading frames in the 5′ region of the ATF4 mRNA [30]. ATF4 controls expression of a wide range of genes that allow adaptation of cells to stressful surroundings to promote cell survival, e.g. via induction of autophagy, but—depending on the context—can also induce apoptosis [31].

Based on our observation that XRCC1-depletion caused wide-ranging anabolic changes in cellular metabolism, we hypothesised that the downregulation of BER in response to persistent stressful influences could enhance cellular survival under suboptimal conditions, such as nutrient restriction. Here, we demonstrate that persistent DNA damage, caused by a decrease in BER capacity or direct induction of DNA damage, triggers activation of the ISR pathway through ATM, PERK, peIF2α, and ATF4 to enhance cellular survival under nutrient-restricted conditions. Our results uncover a previously unappreciated connection between the BER capacity, persistent DNA damage signalling, and ISR, constituting a novel mechanism to support cell survival in response to genotoxic stress that has strong implications for tumour biology and beyond.

Results

XRCC1 KD imparts human fibroblasts with a survival advantage in nutrient-restricted conditions

Why do persistently stressed cells lower the expression of XRCC1? Based on our previous findings, we hypothesised that the downregulation of BER capacity would lead to a metabolic rewiring towards nutritional self-

sufficiency that would be advantageous for cells to survive under nutrient-starved conditions. To test this hypothesis, Tig-1 human primary fibroblasts were treated with XRCC1 or control siRNA and reseeded into dishes with medium containing varying amounts of foetal calf serum (FCS) 24 h later. Cell morphology and density were analysed 72 h after knockdown (KD) using phase-contrast images. When grown in a medium containing 15 or 5% FCS, no obvious differences in cell number or morphology were discernible between XRCC1 KD and control cells (Fig. 1a, b, e, and Additional file 1, Figure S1A and B). Interestingly, however, when FCS was lowered to 1%, XRCC1 KD cells clearly displayed a significantly higher cell number, a more elongated fibroblast-like cell morphology, and less rounded and floating cells compared to controls (Fig. 1c, d, e). KD efficiency and transcriptional response of known genes upregulated in response to XRCC1 KD (ACTA2, PALLD [26]) were not affected by reseeding cells into the different FCS conditions (Additional file 1, Figure S1C). These results were validated using two additional siRNA sequences against XRCC1 (Additional file 2, Figure S2) and in two other human primary fibroblast cell lines (Additional files 3 and 4, Figures S3 and S4). The

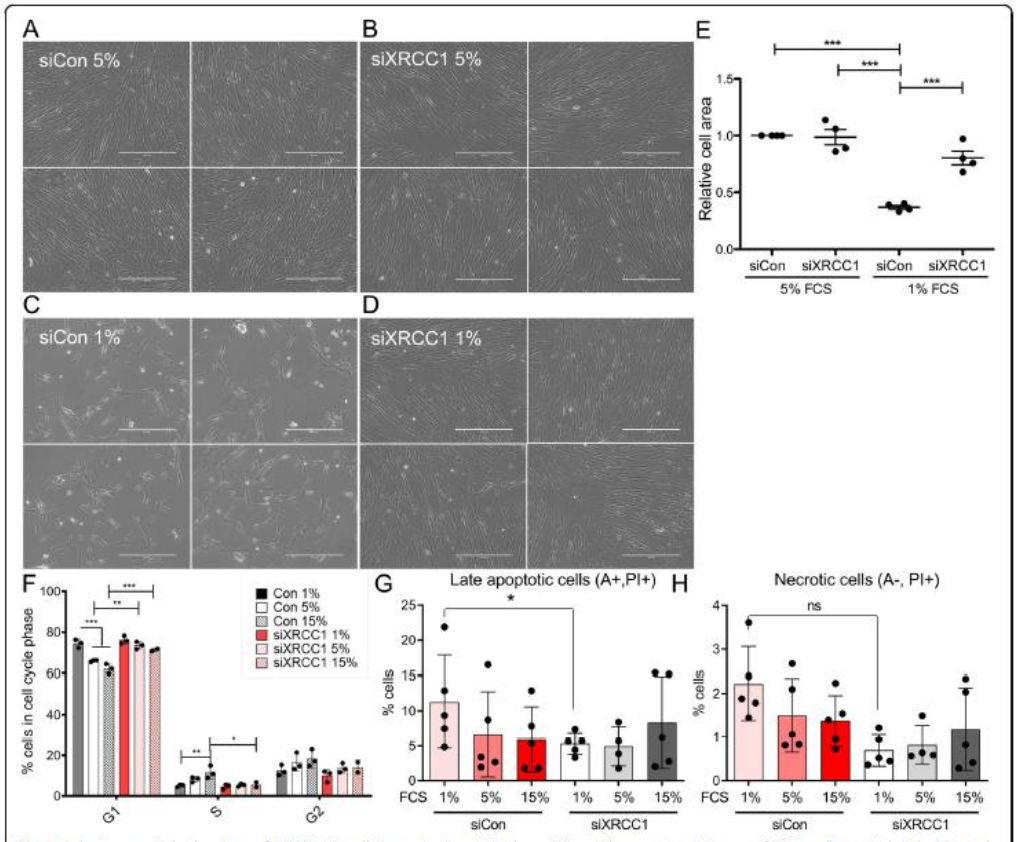

Fig. 1 Selective survival advantage of XRCC1 KD cells in nutrient-restricted conditions. Phase-contrast images of Tig-1 cells treated with siControl (**a**, **c**) or siXRCC1 (**b**, **d**) and grown in a medium containing 5% FCS (**a**, **b**) or 1% FCS (**c**, **d**). Images are from one representative experiment, with four different fields randomly chosen per condition. Scale bar = 400 μm. **e** Quantification of relative cell area as shown in **a**–**d**, normalised to siControl grown at 5% FCS. $n = 4$. Only statistically significant differences are indicated using asterisks. **f** Cell cycle analysis of siControl and siXRCC1 cells cultured at 15%, 5%, and 1% FCS, respectively. Shown is the percentage of cells in the respective cell cycle phases. $n = 3$. Statistically significant differences are indicated using asterisks. **g** Quantification of the percentage of cells in late apoptosis in siControl and siXRCC1 cells cultured at 15%, 5%, and 1% FCS, respectively. $n = 3$. $^*p < 0.05$. **h** Quantification of the percentage of necrotic cells in siControl and siXRCC1 cells cultured at 15%, 5%, and 1% FCS, respectively. $n = 3$. n.s. not significant

increased cell number of XRCC1 KD cells under low FCS conditions could be due to either an increase in proliferation, a decrease in apoptosis, or a combination of both. To differentiate between these possibilities, we analysed the cell cycle distribution of control and XRCC1 KD cells grown in 1%, 5%, and 15% FCS, respectively, using flow cytometry. As expected from previous findings [28], XRCC1 KD cells grown at 15% FCS displayed a significant increase in G1 cells and a concomitant decrease in S-phase cells compared to controls, suggesting that XRCC1 KD under these conditions causes the cell cycle to slow down slightly by prolonging the G1-phase, presumably due to the accumulation of persistent DNA damage (Fig. 1f). Similarly to this, cell cycle distribution at 5% still displayed significantly more XRCC1 KD cells in G1 and slightly less in S-phase compared to control cells. However, in cells grown at 1% FCS, no differences in the percentage of cells in G1, S, or G2 cell cycle phases could be detected between control and XRCC1 KD cells. Indeed, the amount of control cells in G1 significantly increased and cells in S-phase significantly decreased with lower FCS concentrations, while the percentage of XRCC1 KD cells in the different cell cycle phases remained stable throughout the different FCS conditions. Thus, XRCC1 KD cells did not have a proliferative advantage over control cells at low FCS conditions. To understand whether apoptosis differed between control and XRCC1 KD cells grown in low FCS, we analysed the rate of apoptotic cells by Annexin V/propidium iodide staining at 72 h after seeding into different FCS-containing media. While no significant changes between control and siXRCC1 cells at 15% and 5% FCS could be detected, there were significantly more late apoptotic control cells than siXRCC1 cells when cultured at 1% (Fig. 1g). A similar trend was observed with respect to necrotic cells, but this difference did not reach statistical significance (Fig. 1h). Of note, these values are likely to strongly underestimate the real amount of dying cells in the control situation, since most of the dead cells are already lost before the analysis (Fig. 1c, d). The observed increase in apoptotic cell death of control cells is also in accordance with the phenotype, as the control clearly shows much more rounded, detaching, and floating cells than the XRCC1 KD (Fig. 1c, d). In summary, these results strongly support the hypothesis that XRCC1 KD confers cells with a survival advantage in nutrient-restricted conditions.

XRCC1 KD induces the integrated stress response through PERK-peIF2α-ATF4 signalling to support cell survival in nutrient-restricted conditions

BER depletion in fibroblasts through KD of XRCC1 has been shown to induce transcription of ATF4 by a yet unknown mechanism [26, 28]. ATF4 is a transcription factor that can induce metabolic adaptations to stressful conditions and thereby promote survival [29–31]. Therefore, we asked whether the survival advantage of fibroblasts in nutrient-restricted conditions upon XRCC1 KD depended on ATF4. At 5% FCS, depletion of ATF4 alone or in combination with XRCC1 merely showed a slight decrease in cell numbers compared to control cells, suggesting that a baseline ATF4 level is required for optimal cellular fitness (Additional file 5, Figure S5A-D). Strikingly, when cultured at 1% FCS, combined KD of ATF4 and XRCC1 completely rescued the phenotype observed with XRCC1 KD alone and was virtually indistinguishable from control cells (Fig. 2a–e). KD efficiency was not influenced by FCS conditions, and functionality of the ATF4 KD was further validated by a strong decrease in expression of PSAT1, a known direct downstream target of ATF4, as well as rescue of ACTA2 and PALLD expression, which are known to be upregulated after XRCC1 KD through an ATF4-dependent mechanism (Fig. 2f) [26]. It is important to note that these XRCC1 KD-induced changes on both transcript and protein levels could be observed irrespective of the FCS conditions, but the phenotype of increased survival over control cells only manifested upon FCS restriction (Fig. 2f and data not shown). We conclude that increased cell survival upon XRCC1 KD under nutrient-restricted conditions depends on the transcription factor ATF4.

As a central effector of the ISR, ATF4 can be regulated on the translational level by activation of the ISR [30]. To determine whether XRCC1 KD resulted in an increase in ATF4 protein levels, we analysed ATF4 levels in XRCC1 KD cells. Western blot analysis revealed a strong increase of ATF4 protein upon XRCC1 KD (Fig. 3a), which was further validated using two other siRNA sequences against XRCC1 (Additional file 5, Figures S5E and F). We next wondered whether XRCC1 KD could induce phosphorylation of eIF2α (peIF2α) and thereby increase ATF4 translation through activation of the ISR. In line with an increase in ATF4 translation through activation of the ISR by XRCC1 KD, Western blot analysis confirmed that XRCC1 KD induced peIF2α (Fig. 3b). Of note, the extent of peIF2α activation by XRCC1 KD was comparable with its induction by the known ER-stress inducer Thapsigargin. These results prompted the question, which of the upstream kinases was responsible for XRCC1 KD-mediated activation of the ISR that led to upregulation of ATF4. GCN2 and PERK have been shown to be important in response to amino acid and glucose starvation as well as endoplasmic reticulum stress [32]. While ATF4 upregulation upon XRCC1 KD was not altered by co-KD of GCN2 (Fig. 3c and Additional file 5, Figure S5G), co-KD of PERK completely abrogated ATF4 induction (Fig. 3d). Importantly, co-KD of PERK with XRCC1 also annulled the increased survival of XRCC1 KD cells at 1% FCS (Fig. 3e–i). Similar results were obtained by inhibition of

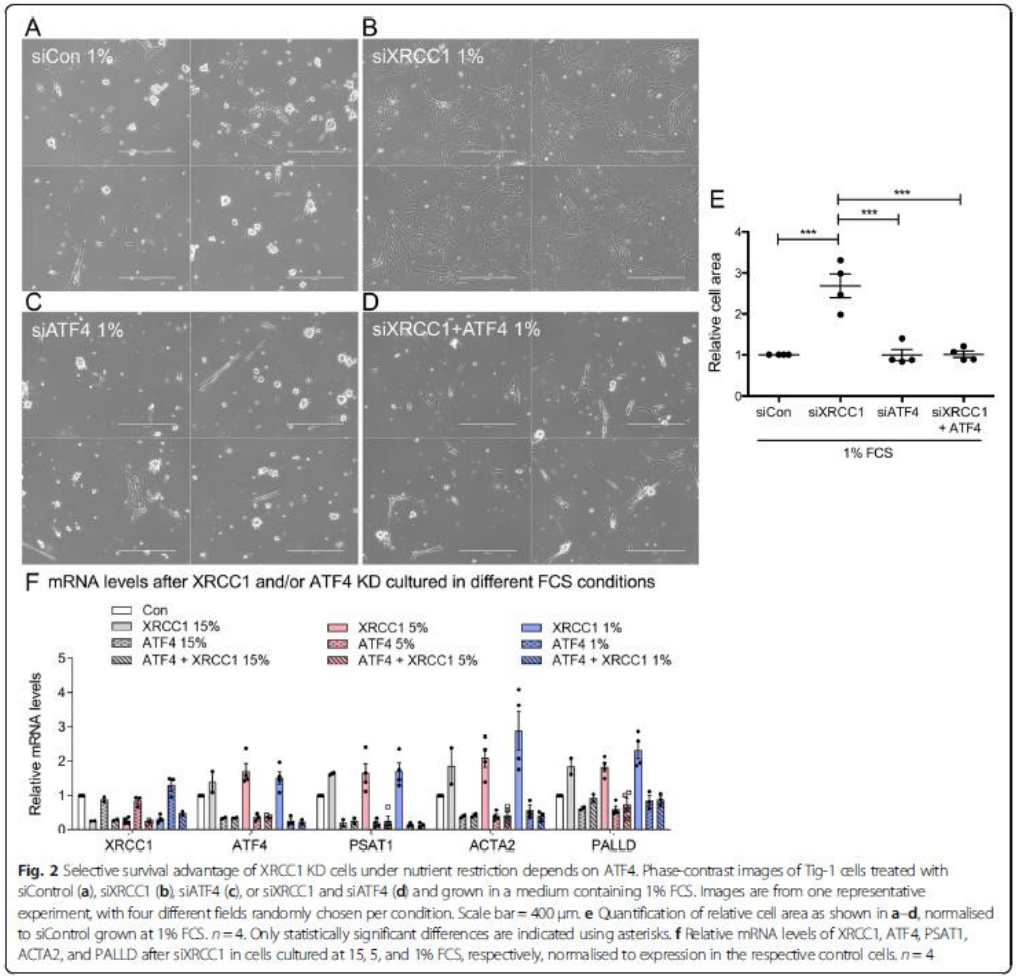

Fig. 2 Selective survival advantage of XRCC1 KD cells under nutrient restriction depends on ATF4. Phase-contrast images of Tig-1 cells treated with siControl (**a**), siXRCC1 (**b**), siATF4 (**c**), or siXRCC1 and siATF4 (**d**) and grown in a medium containing 1% FCS. Images are from one representative experiment, with four different fields randomly chosen per condition. Scale bar = 400 μm. **e** Quantification of relative cell area as shown in **a**–**d**, normalised to siControl grown at 1% FCS. $n = 4$. Only statistically significant differences are indicated using asterisks. **f** Relative mRNA levels of XRCC1, ATF4, PSAT1, ACTA2, and PALLD after siXRCC1 in cells cultured at 15, 5, and 1% FCS, respectively, normalised to expression in the respective control cells. $n = 4$

PERK using GSK2606414 in combination with XRCC1 KD (Additional file 6, Supplementary Figure S6) [33]. Hence, these findings suggest that XRCC1 KD-mediated activation of the ISR proceeds through the PERK-peIF2α-ATF4 signalling pathway, which manifests in a survival advantage of cells under nutrient restriction.

The XRCC1 KD-induced survival advantage in nutrient-restricted conditions is induced through signalling of persistent DNA single-strand breaks via ATM

Given the connection between depletion of XRCC1 and the survival advantage in nutrient-restricted conditions mediated through activation of the ISR, we sought to identify the mechanism by which XRCC1 KD could induce the ISR. It is well established that XRCC1 KD induces persistent DNA damage due to BER deficiency, which leads to poly-ADP-ribose (PAR) formation [7, 8, 25, 26, 28, 34, 35]. In line with this, XRCC1 KD cells displayed an increase in persistent DNA damage as measured by the alkaline comet assay (Fig. 4a), increased PAR formation (Fig. 4b), and phosphorylation of ATM (Fig. 4c). Importantly, consistent with previous reports [35], XRCC1 KD Tig-1 cells did not accumulate DSBs as evidenced by a lack of increase in γH2AX by Western blot (Fig. 4d), no increase in DSBs as assessed by the neutral comet assay (Fig. 4e), and no change in the number of 53bp1 or γH2AX foci in the cell nuclei (Fig. 4f, g). Therefore, we asked whether DNA damage signalling was involved in the activation of the ISR upon XRCC1 KD. SSBs

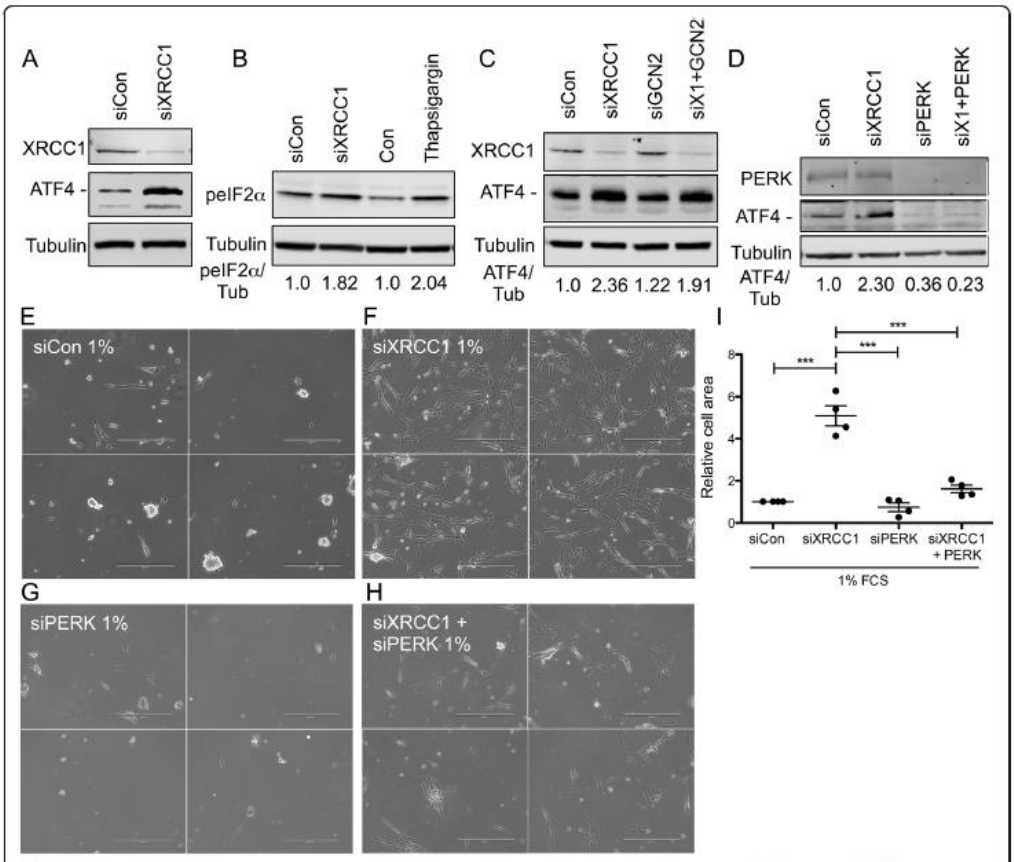

Fig. 3 XRCC1 KD induces the integrated stress response through PERK to support survival under nutrient-restricted conditions. **a**–**d** Representative Western blots of **a** ATF4 and XRCC1 levels after siXRCC1. The band specific for ATF4 is indicated with a dash. $n = 3$. **b** peIF2α after siXRCC1 or Thapsigargin. Normalised peIF2α levels are shown below the lanes. $n = 3$. **c** ATF4 and XRCC1 after KD of XRCC1 and/or GCN2. The band specific for ATF4 is indicated with a dash. Normalised levels of ATF4 are shown below the lanes. $n = 3$. **d** PERK and ATF4 after KD of XRCC1 and/or PERK. The band specific for ATF4 is indicated with a dash. Normalised levels of ATF4 are shown below the lanes. $n = 3$. **e**–**h** Phase-contrast images of cells treated with **e** siControl, **f** siXRCC1, **g** siPERK, or **h** siXRCC1 and siPERK, and grown in medium containing 1% FCS. Images are from one representative experiment with four different fields randomly chosen per condition. Scale bar = 400 μm. **i** Quantification of relative cell area as shown in **e**–**h**, normalised to siControl grown at 1% FCS. $n = 4$. Only statistically significant differences are indicated using asterisks

and DNA base damage have been shown to induce signalling through PARP, ATM, and DNA PK_{cs} [35–37]. Neither inhibition of DNA PK_{cs} nor PARP using two different inhibitors could rescue the increase in ATF4 expression upon XRCC1 KD (Fig. 4h, i, and Additional file 7, Figure S7A). In contrast, inhibition of ATM was able to rescue the induction of ATF4 (Fig. 4j and Additional file 7, Figure S7B). ATM inhibition also rescued the increase in peIF2α upon XRCC1 KD (Fig. 4k). Importantly, while not affecting growth at 5% FCS, ATM inhibition completely rescued the increased survival imparted by XRCC1 KD at 1% FCS (Fig. 4l–p and Additional file 7, Figure S7C). Thus, increased survival in nutrient-restricted conditions through activation of the ISR by XRCC1 KD depends on signalling of SSBs by ATM.

Manipulation of the XRCC1 transcription factor Sp1, single-strand breaks induced by low-level H_2O_2, and DNA double-strand breaks induced by ionizing radiation also activate the ISR-mediated cell survival under nutrient-restricted conditions

We then wondered whether activation of the ISR could also be triggered by other modalities that lead to a

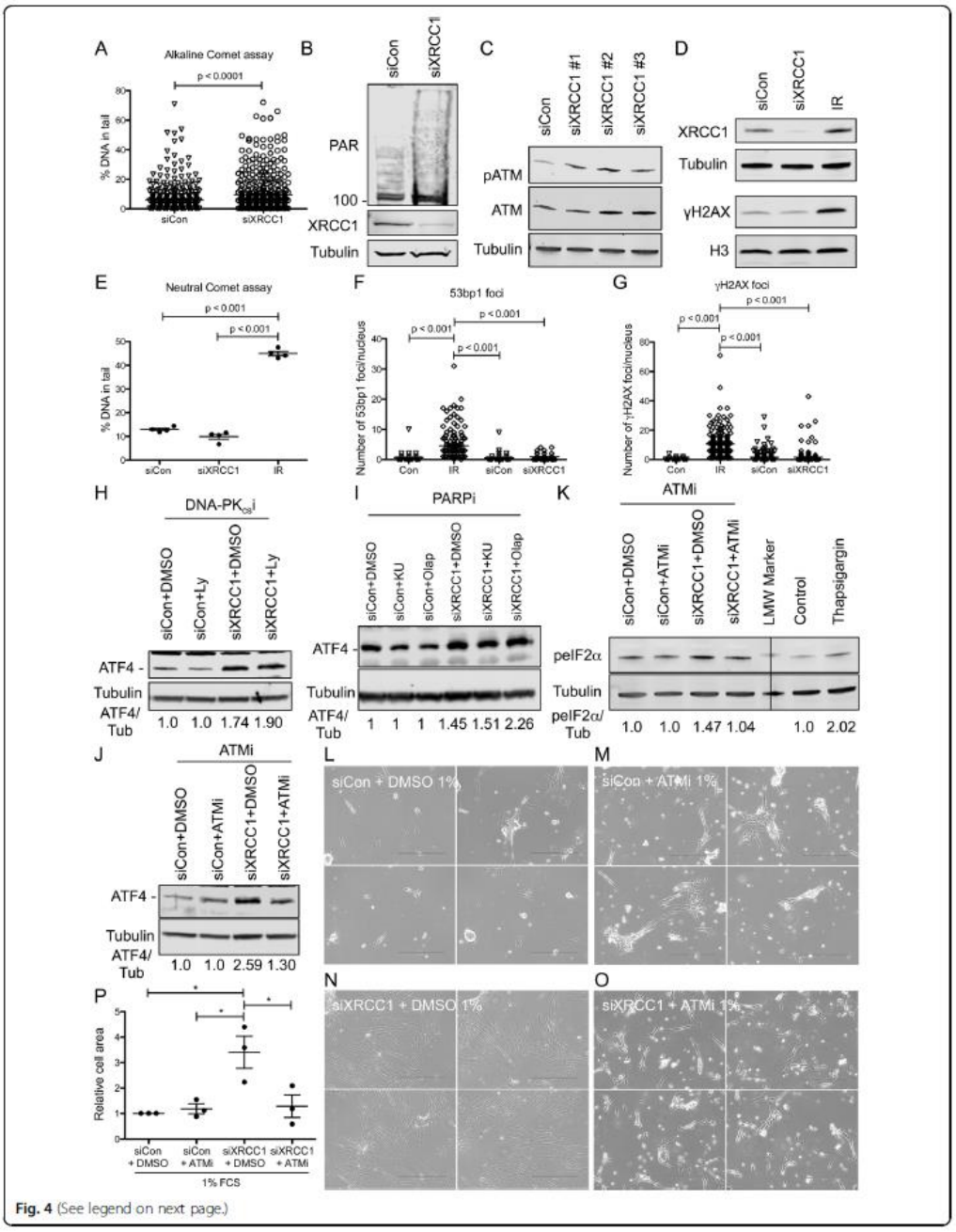

Fig. 4 (See legend on next page.)

(See figure on previous page.)
Fig. 4 The XRCC1 KD-induced activation of the ISR is mediated through signalling of persistent single-stranded DNA damage via ATM. **a** Alkaline comet assay of siControl and siXRCC1 cells. **b**–**d** Representative Western blots of **b** PAR and XRCC1 after siXRCC1. The smear above 100 kDa marker indicates PAR. **c** pATM and ATM after siXRCC1 using 3 different siRNA sequences. **d** γH2AX, Histone H3, XRCC1, and Tubulin in cells after siXRCC1, or 4 Gy IR. **e** Neutral comet assay of cells treated after siControl, siXRCC1, or 4 Gy IR. $n = 4$. **f**, **g** Quantification of 53 bp1 (**f**) or γH2AX (**g**) foci per nucleus in cells after 4 Gy IR, siControl, or siXRCC1. **h**–**j** Representative Western blots of **h** ATF4 in siControl or siXRCC1 cells treated with Ly or DMSO; **i** ATF4 in siControl or siXRCC1 cells treated with KU, Olap, or DMSO; **j** ATF4 in siControl or siXRCC1 cells treated with ATMi or DMSO; and **k** peIF2a in siControl or siXRCC1 cells treated with ATMi or DMSO. Normalised levels of ATF4 or peIF2α are shown below the lanes. **l**–**o** Phase-contrast images of siControl (**l**, **m**) or siXRCC1 (**n**, **o**) cells treated with DMSO (**l**, **n**) or ATMi (**m**, **o**), grown in a medium containing 1% FCS. Images are from one representative experiment, with four different fields randomly chosen per condition. Scale bar = 400 μm. **p** Quantification of relative cell area as shown in **l**–**o** normalised to siControl + DMSO grown at 1% FCS. $n = 3$. For all quantifications, only statistically significant differences are indicated using asterisks

decrease in XRCC1 levels. Expression of XRCC1 is controlled by the transcription factor Sp1, and depletion of Sp1 leads to a deficiency in BER due to decreased transcription of XRCC1 [27]. Consistent with this, KD of Sp1 for 72 h led to a significant reduction of XRCC1 protein levels, as well as an increase in pATM, supporting the notion that Sp1 KD leads to persistent DNA damage due to a depletion in XRCC1 protein levels (Fig. 5a). Of note, Sp1 KD did not elevate γH2AX levels (Fig. 5b). Accordingly, Sp1 KD also triggered an increase in both ATF4 and peIF2α levels (Fig. 5c), suggesting that the transcriptional downregulation of XRCC1 of approximately 40% (Fig. 5a) obtained by KD of Sp1 is sufficient to trigger activation of the ISR. In line with this, Sp1 KD cells displayed significantly increased survival compared to siControl-treated cells when cultured at 1% FCS, but not at 5% FCS (Fig. 5d–f, Additional file 8, Figure S8A and B).

Next, we asked if the observed phenomenon could also be elicited by direct induction of persistent DNA damage. For this, we analysed ATF4 and peIF2α levels in cells exposed to low levels of hydrogen peroxide (H_2O_2) for 72 h, which caused a slight increase of SSBs compared to control cells (Fig. 5g), but failed to induce DSBs as assessed by the neutral comet (Fig. 5h) and γH2AX levels (Fig. 5i). Exposure of cells to 25 or 50 μM H_2O_2 over 72 h led to an upregulation of ATF4 and peIF2α protein, in accordance with an induction of the ISR by persistent DNA damage (Fig. 5j). Of note, this treatment also precipitated a decrease in XRCC1 protein levels (Fig. 5j). Strikingly, such chronic exposure to low levels of H_2O_2 before seeding into low FCS medium induced a significant survival advantage in these cells compared to control treated cells upon culture at 1% FCS (Fig. 5k–n). Hence, persistent single-strand DNA damage brought about by chronic exposure to low levels of H_2O_2 induces an ISR-dependent selective survival advantage under nutrient-restricted conditions.

Finally, since ATM is well-known to be activated upon DSB formation by ionising radiation [38], we wondered whether its activation by direct formation of DSBs could also induce the ISR. Indeed, Tig-1 cells irradiated for three consecutive days with doses of 0.5, 1, or 2 Gy, respectively, displayed elevated levels of pATM as well as peIF2α and ATF4 (Fig. 5o). Importantly, cells pretreated in this way with ionising radiation before reseeding also displayed increased survival upon culture in 1% FCS compared to control cells (Fig. 5p–t). From these results, we conclude that activation of ATM through DSBs also leads to induction of the ISR to support cell survival under nutrient restriction.

Collectively, our data clearly demonstrate that persistent DNA damage, as induced via downregulation of XRCC1 or direct induction of SSBs or DSBs through DNA-damaging agents, confers cells with a selective survival advantage in nutrient-restricted conditions through an ATM-dependent activation of the ISR pathway involving the PERK-peIF2α-ATF4 axis. As such, these results uncover a previously unappreciated connection between the BER capacity, DNA damage signalling, and the ISR, which supports cell survival in response to genotoxic stress with strong implications for tumour biology and other physiological conditions in which cells have been shown to selectively decrease the levels of BER components.

Discussion

As a mainstay of genome integrity, BER is a centrally important pathway to counteract DNA lesions that arise due to constant exposure of living organisms to exogenous and endogenous DNA-damaging agents. Hence, tight adaptation of BER capacity to cellular needs is considered critically important, as both insufficient or uncontrolled repair activity could potentially lead to the accumulation of DNA damage and mutations [6, 24, 25, 39]. Under most physiological circumstances, BER capacity is sufficient to avoid accumulation of unrepaired DNA damage. Acute genotoxic stress could lead to temporal exhaustion of BER capacity, leading to delays in repair of DNA damage, potentially giving rise to genetic instability. Importantly, however, there are also numerous physiological circumstances in which cells have been described to selectively induce a BER deficiency [40–44]. While the general idea has been that downregulation of

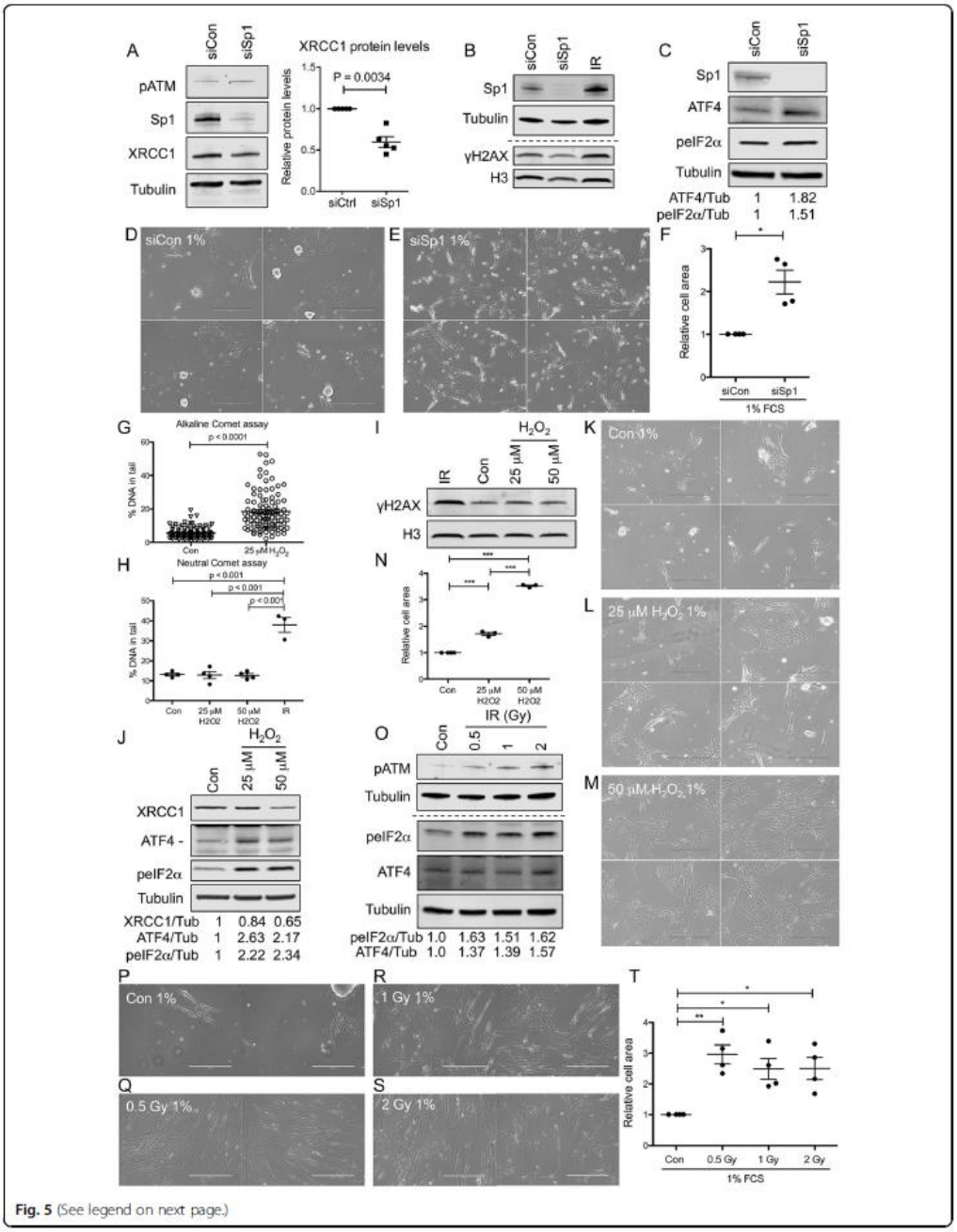

Fig. 5 (See legend on next page.)

(See figure on previous page.)
Fig. 5 Induction of ISR-mediated cell survival under nutrient-restricted conditions through KD of Sp1, direct SSBs induced by H_2O_2, or direct DSBs induced by ionising radiation. **a** (left) Representative Western blot of pATM, Sp1, and XRCC1 levels after siSp1. (right) Quantification of XRCC1 levels shown on the left, $n = 5$. **b**, **c** Representative Western blot of **b** Sp1, Tubulin, γH2AX, and Histone H3, or **c** Sp1, ATF4, and pelF2α after siSp1. Normalised levels of ATF4 and pelF2α are indicated. **d**–**e** Phase-contrast images of cells treated with siCon (**d**) or siSp1 (**e**), grown in a medium containing 1% FCS. **f** Quantification of **d** and **e**, $n = 4$. **g** Alkaline comet assay of cells treated with 25 μM H_2O_2. **h** Neutral comet assay of cells pre-treated with 25 μM or 50 μM H_2O_2 for three consecutive days, or 4 Gy IR 15 min prior to harvesting, respectively. $n = 4$. **i**, **j** Representative Western blots of **i** γH2AX and Histone H3 or **j** XRCC1, ATF4, and pelF2α, in cells treated as in **h**. Normalised levels of XRCC1, ATF4, and pelF2α are indicated. **k**–**m** Phase-contrast images of cells treated as in **h** prior to seeding into a medium containing 1% FCS. **n** Quantification of **k**–**m**. $n = 4$. **o** Western blot of pATM, Tubulin, ATF4, and pelF2α in control cells or cells treated with 0.5, 1, or 2 Gy of IR on three consecutive days. Normalised levels of ATF4 and pelF2α are indicated. **p**–**s** Phase-contrast images of control cells (**p**) or cells treated as in **o** prior to seeding into a medium containing 1% FCS. **t** Quantification of **p**–**s**, $n = 4$

BER in these cells might 'prime' them for apoptosis or removal by the immune system, evidence for this is still inconclusive. Indeed, several aspects suggest a physiological role for this transient attenuation of BER capacity that goes beyond simple priming of cells for apoptosis and removal, as outlined in the following. Circulating monocytes have been shown to harbour a deficiency in DNA repair due to downregulation of key repair proteins [40, 45, 46]. However, dendritic cells or macrophages that are derived from these monocytic precursors re-express the relevant repair proteins, becoming repair-proficient again. It would quite simply not make much sense to try and initially target all of these precursor cells by default for apoptosis or removal by the immune system as a step during their maturation even before they have reached their final differentiation state. Similarly, chronic hypoxia has been found to lead to a decrease in expression of several BER proteins, and human spermatozoa harbour a 'truncated BER pathway' manifested by the absence of XRCC1 and Ape1 [44]. Finally, human primary fibroblasts that are exposed to prolonged treatments with pro-inflammatory cytokines or oxidative stress strongly decrease their BER capacity due to a downregulation of XRCC1 and other BER proteins [25–27]. Importantly, human fibroblasts are considered highly apoptosis-resistant, and to undergo senescence much rather than apoptosis, and they can be maintained in culture for extremely long periods in that state [47]. This is in line with the crucial role of fibroblasts to maintain the organism's structural integrity, because, even in a post-replicative senescent state, fibroblasts are still able to actively shape the extracellular matrix. This would not be possible where damaged fibroblasts are quickly eliminated through apoptosis or by the immune system. Following up on the idea that the specific downregulation of BER capacity could serve a physiological purpose, our work uncovers a previously unappreciated connection between the BER, persistent DNA damage, and the ISR that supports cell survival in response to genotoxic stress. These findings have strong implications for tumour biology in a variety of aspects. On the one hand, these results could directly impact on cells in the tumour microenvironment, the so-called cancer-associated stroma, and especially cancer-associated fibroblasts (CAFs), which are highly central players in the development and progression of tumours [48, 49]. Here, persistent DNA damage signalling could increase survival and self-sufficiency of stromal tumour-supportive cells. Interestingly, ROS has been shown to be a potent inducer of CAFs [50]. In line with this, we have shown that persistent DNA damage in fibroblasts leads to a secretory phenotype by which fibroblasts are able to support growth and metastatic ability of tumour cells [26]. Thus, we propose that under stressful circumstances, such as protracted inflammation or persistent ROS, DNA damage is induced in the tissue-resident fibroblasts, which leads to ATM signalling that initiates ATF4-dependent metabolic reprogramming to increase cellular self-sufficiency in nutrients, thereby enabling these cells to survive even in nutrient-starved conditions. Through this increased resilience, fibroblasts can still fulfil their important structural roles in the organism, as they are the main responsible for synthesis of the extracellular matrix, that provides the structural scaffold for other cells to grow on and mechanical properties that determine the integrity of organs [51]. Such a resilience mechanism seems important especially also for CAFs. *Per definitionem*, CAFs are located closely adjacent to the epithelial tumour-forming, rapidly dividing cancer cells. These cancer cells have a huge demand in a wide variety of nutrients to sustain their high proliferative rate, and they have been shown to remodel the surrounding stroma in a way that increases the delivery of such nutrients and other growth-promoting molecules [48]. Specifically, CAFs have been found to take up metabolic waste of cancer cells to produce metabolites that in turn are secreted again to feed the tumour [52]. It is thus thought that most of the 'rich' nutrients are drained away from CAFs to support tumour growth, which results in the necessity for CAFs to survive in a 'starved' environment. The observed downregulation of BER capacity in fibroblasts exposed to a maintained pro-inflammatory stimulation that induces CAF generation seems to thus increase self-sufficiency of these cells, which would be beneficial in a starved environment. In summary, our observations suggest the metabolic rewiring upon BER decline

after stressful insults to be a physiological response of fibroblasts to ensure their survival in nutrient-starved conditions, in order to fulfil their principal role of maintaining the structure of the organism. On the other hand, our findings could also have implications for survival of premalignant or malignant tumour cells, which are strongly exposed to various different types of stress [31]. However, the reaction of tumour cells to persistent DNA damage with regard to activation of the ISR and their survival under nutrient starvation remains to be addressed in the future.

Mechanistically, we found activation of the ISR by XRCC1 depletion to depend on signalling of SSBs via ATM, which activates PERK-mediated eIF2α phosphorylation and increases translation of the transcription factor ATF4 (Figs. 3 and 4). Currently, it remains unclear whether activation of PERK by ATM is direct or indirect. Additionally, also other modalities that induced SSBs (Sp1 KD and treatment with low levels of H_2O_2) and even direct induction of DSBs using ionising radiation led to the activation of the ISR-mediated survival phenotype (Fig. 5). Interestingly, cell death that is observed under acute exposure of control cells to nutrient-starved conditions very much resembles the 'foamy cell death' that has recently been described in response to chronic ER stress [53]. Prevention of this form of cell death also depends on PERK activation of peIF2α, similarly to what we observe upon XRCC1 KD. Additionally, this foamy cell death apparently seems to be driven by a 'non-apoptotic' mechanism, which would explain why the quantification of apoptotic cells through Annexin V-PI staining does fully recapitulate the extent of cell death that is visible under nutrient-deprived conditions in control cells (Fig. 1). Indeed, it seems that the Annexin V-PI staining only captures a very small proportion of the effect that acute nutrient starvation has on the control cells. It will be interesting to determine what exact mechanism precipitates cell death under these conditions.

The transcription factor ATF4 has a dual role in cells promoting either their adaptation to endure stress or the induction of apoptosis [31]. The ATF4 dependence of the metabolic reprogramming that we observed upon both XRCC1 KD and induction of DSBs is nicely in line with our previous findings demonstrating increased ATF4 transcription after XRCC1 KD [28] as well as its involvement in the transcription of several CAF markers that are activated upon XRCC1 KD [26]. Hence, cells with persistent DNA damage seem somehow to be able to exploit ATF4, to reduce stress resulting from nutrient limitation and benefit from its pro-survival effects. This raises intriguing questions as to what exact ATF4-dependent changes allow cells to thrive in nutrient-starved conditions and why ATF4 promotes cellular survival after persistent DNA damage under these conditions rather than inducing apoptosis. A deeper understanding of these mechanisms might also facilitate the identification of pharmacological strategies to fine-tune ATF4 activity in different pathologies, such as cancer.

Conclusion

Our results uncover a previously unappreciated connection between persistent DNA damage, caused either by a decrease in BER capacity or by direct induction of DNA single-strand or double-strand breaks, and activation of the ISR. Activation of the ISR by DNA damage relies on phosphorylation of the DNA damage sensor protein ATM, which leads to PERK-mediated eIF2α phosphorylation, increasing translation of the stress-response factor ATF4. This mechanism supports cell survival in response to genotoxic stress with strong implications for tumour biology and beyond.

Methods

Cell culture

TIG-1, AG09319, and AG16409 primary human fibroblasts were purchased from Coriell and cultured under standard conditions (37 °C, 5% CO_2) in Gibco™ DMEM, low glucose, GlutaMAX™ Supplement, pyruvate containing 15% foetal calf serum (FCS). For all treatments using inhibitors, inhibitors were dissolved in DMSO, medium was changed, and fresh inhibitor was added every 24 h. The following inhibitors were used: PERKi GSK2606414 (MerckMillipore), used at 1 μM final concentration; DNA-PK_{cs}i LY294002 (Ly, MerckMillipore), used at 1 μM final concentration; ATMi Ku-60019 (ATMi, SigmaAldrich), used at 10 μM final concentration; and PARPi Ku-0058948 (Ku; AxonMedChem) and Olaparib (Olap; Selleck Chemicals), both used at 1 μM final concentration. As positive control to induce ER stress/peIF2α/ATF4, cells were exposed for 3 h to 1 μM Thapsigargin (Sigma). To induce DNA double-strand breaks, cells were irradiated using a Faxitron Cabinet X-ray system Model RX-650 at the indicated IR doses.

siRNA transfection

Transfections with siRNA purchased from Eurogentec or Thermo Fisher were carried out using Lipofectamine RNAiMAX reagent (Invitrogen) according to the manufacturer's specifications. Cells were analysed at indicated time points after transfection. siRNA sequences used are listed in Additional file 9, Table S1.

Analysis of cell growth in serum-restricted growth conditions

10^6 cells were seeded into 10-cm dishes 24 h prior to siRNA transfection in standard medium containing 15% FCS. Twenty-four hours after transfection, cells were washed and trypsinised with 1 ml trypsin solution, and trypsin was neutralised through addition of 2 ml of

DMEM containing 5% FCS. One ml of the cell solution was distributed into each fresh 10-cm dish, containing 10 ml of medium with different concentrations of FCS (i.e. 15, 5, and 1%), and incubated another 72 h until analysis. Images of random fields were obtained with a phase-contrast microscope at ×10 magnification, and cells were collected for further analysis. For experiments involving pre-treatment of cells with H_2O_2 or IR, cells were grown in 10-cm dishes in standard medium containing 15% FCS for the duration of the pre-treatment. Pre-treatment was performed thrice every 24 h using the indicated doses of H_2O_2 or IR. For treatments with H_2O_2, the medium was changed every time. Twenty-four hours after the third round of pre-treatment, equal numbers of cells were seeded into different FCS-containing dishes as described above. To quantify the relative cell area from phase-contrast images, the area covered with cells was quantified after thresholding of images to remove the background using ImageJ software. For each experiment and data point, two to four independent fields were quantified, and mean values were calculated, which were then normalised to the respective control. Every experiment was independently repeated three to four times ($n = 3$ or 4), as indicated in the respective figure legends. Data are expressed as individual data points and mean ± SEM. Raw data can be found in Additional file 12 Table S4.

qRT-PCR

Total RNA was purified using the RNeasy® Mini Kit by QIAGEN according to the manufacturer's protocol. Equal amounts of RNA were reverse transcribed using the BioRad iScript™ cDNA Synthesis Kit according to the manufacturer's protocol with the LabCycler (SensoQuest). Quantitative real-time PCR (RT-qPCR) was performed using the KAPA SYBR® FAST One-Step qRT-PCR Kit in a total volume of 10 µl in duplicates on the CFX384 Touch™ Real-Time PCR detection system (Bio-Rad). The comparative CT method was applied for quantification of gene expression, values were normalised against GAPDH and B2M and the control, and results were expressed as fold change in mRNA levels over control cells. Each experiment was independently repeated between two and four times as indicated in the figure legends, and data are expressed as individual data points and mean ± SD. Primers are detailed in Additional file 10 [54], Table S2, and were ordered from Microsynth. Raw data can be found in Additional file 12, Table S4.

Flow cytometry

For cell cycle analysis by FACS, trypsinised cells were fixed in ice-cold 70% ethanol for at least 30 min at −20 °C. To remove the fixation solution, cells were spun 5 min at 250 rcf at 4 °C, and the supernatant was discarded. Cells were then resuspended in phosphate-buffered saline with 100 µg/ml of DNase free RNase A (Sigma) and incubated at 37 °C for 30 min and further stained with 10 µg/ml propidium iodide (Sigma). Samples were run on a Fortessa (BD Biosciences) and the cell cycle distribution analysed using FlowJo V10.6.1. Each experiment was independently repeated three times. Data are mean ± SD of $n = 3$ independent experiments and are expressed as individual data points and mean ± SD. Analysis of apoptotic and necrotic cells was performed with the Annexin V-FITC Apoptosis Staining/Detection Kit (Abcam, ab14085) according to the manufacturer's protocol. Briefly, cells treated as indicated were washed and adherent cells trypsinised. Trypsin was neutralised using serum containing medium, and 500,000 cells were collected by centrifugation and resuspended in 500 µl 1X Binding Buffer. Five µl of Annexin V-FITC and 5 µl propidium iodide were added, and samples were incubated at room temperature for 5 min before acquisition with FACS as detailed above. Each experiment was independently repeated five times. Data are mean ± SD of $n = 5$ independent experiments and are expressed as individual data points and mean ± SD. Raw data can be found in Additional file 12 Table S4.

Western blot

For Western blotting, unless otherwise stated, whole cell extracts that were prepared from cells grown in 15% FCS were used according to a procedure described previously [28]. 20 to 40 µg of total protein extract was separated on 4–20% Tris–Glycine gels (Novex) and transferred onto Immobilon-FL polyvinylidene fluoride (PVDF) membranes (Millipore) according to standard procedures (Novex). Blots were probed with primary antibodies detailed in Additional file 11 Table S3, and secondary antibodies conjugated with Alexa Fluor 680 and IRDye 800CW (both Li-cor Biosciences). Detection and quantification was performed using the Odyssey CLX image analysis system (Li-cor Biosciences). Tubulin or Histone H3 serves as the loading control. Each experiment was independently repeated three to five times. For quantification, protein levels were first normalised to the loading control and then to the respective control lane. Relative protein levels are indicated below the lanes and refer to the blot that is pictured.

Alkaline comet assay

The alkaline comet assay was performed as described [8]. Briefly, cells were harvested by trypsinisation, diluted to a concentration of 2×10^5 cells/ml in medium, and embedded on a microscope slide in 1% low-melting agarose in phosphate-buffered saline (PBS) (Bio-Rad) that was settled on ice. Slides were lysed in buffer containing 2.5 M NaCl, 100 mM ethylenediamine-tetraacetic

acid (EDTA), 10 mM Tris–HCl pH 10.5, 1% (v/v) dimethyl sulfoxide (DMSO), and 1% (v/v) Triton X-100 for 1 h at 4 °C. Slides were then incubated in the dark for 30 min in cold electrophoresis buffer (300 mM NaOH, 1 mM EDTA, 1% (v/v) DMSO, pH > 13) to allow DNA unwinding prior to electrophoresis at 21 V for 25 min in the comet assay tank from Trevigen. Neutralisation of the slides was performed with 0.5 M Tris–HCl (pH 8.0). The slides were stained with SYBR Gold (Invitrogen) and analysed using the Open Comet plugin for Fiji [55]. To quantify, a minimum of 50 cells were analysed per assay and condition, and the assay was repeated independently three to four (Fig. 4) times. All individual data points from all repeats and their mean ± SD are displayed.

Neutral comet assay

The neutral comet assay was performed as described in [56]. Briefly, cell harvesting and embedding was performed as described for the alkaline comet assay. As positive control, cells were irradiated with 4 Gy IR 15 min prior to harvesting. Slides were lysed in buffer containing 2.5 M NaCl, 100 mM EDTA, 10 mM Tris, and 1% *N*-laroylsarcosine, pH 9.5, with freshly added 1% (v/v) DMSO and 0.5% (v/v) Triton X-100 for 1 h at 4 °C in the dark. Slides were then washed 3 times in electrophoresis buffer (300 mM sodium acetate, 100 mM Tris–HCl, pH 8.3) and incubated for 1 h in fresh electrophoresis buffer. Electrophoresis was performed in fresh cold buffer for 1 h at 21 V (ca 120 mA) in the comet assay tank from Trevigen. Afterwards, slides were rinsed 3 times with dH_2O, immediately stained using SYBR Gold (Invitrogen), and air dried. Analysis was performed using the Open Comet plugin for Fiji. For each data point, at least 50 cells were quantified per assay and condition, and mean values were calculated. The experiment was independently repeated 3–4 times. Data are mean ± SD of the mean values from these independent experiments, as indicated in the respective figure legends. Raw data can be found in Additional file 12, Table S4.

Immunofluorescence

Cells were grown in 6-well plates on sterile 12-mm glass coverslips and fixed with 4% paraformaldehyde (pH 8.0) in PBS for 15 min at room temperature. After one wash in PBS, permeabilisation was performed using 0.2% Triton X-100 in PBS for 5 min at room temperature, followed by three washes in PBS. Primary and secondary antibodies were diluted in DMEM with 10% FCS (53 bp1, rabbit, Abcam, 1:1000; γH2AX, mouse, Millipore, 1:1000; anti-mouse Alexa Fluor 488, Thermo Scientific, 1:400; anti-rabbit Alexa Fluor 594, Thermo Scientific, 1:400) and incubated 1–2 h at room temperature. DNA was stained using 4′,6-diamidino-2-phenylindole dihydrochloride (DAPI, 0.2 μg/ml). After 3 washes in PBS, coverslips were mounted on glass slides using ProLong Gold Antifade Mountant (Molecular Probes) and imaged. Automated detection and quantification of foci in nuclei was performed using Fiji. The number of foci was quantified in a minimum of 100 nuclei per condition, with 2 independent repeats. All individual data points from all repeats and mean ± SD are displayed.

Experimental design and statistical analysis

The exact sample size (n) for each experiment is indicated in the respective figure legends. All statistical analysis, calculation, and graphical display were performed with the programme GraphPad Prism (www.graphpad.com). Statistical testing of differences from 3 groups or more was performed using one-way ANOVA followed by Bonferroni's multiple comparison test, while Student's t test was applied when only two groups were compared. Significance levels are $^{*}p < 0.05$, $^{**}p < 0.01$, and $^{***}p < 0.001$.

Supplementary information

Supplementary information accompanies this paper at https://doi.org/10.1186/s12915-020-00771-x.

Additional file 1: Figure S1. No influence of XRCC1 KD in cells grown at 15% FCS.

Additional file 2: Figure S2. Selective growth advantage of XRCC1 KD cells at 1% FCS.

Additional file 3: Figure S3. Selective growth advantage of AG09319 cells after XRCC1 KD at low FCS.

Additional file 4: Figure S4. Selective growth advantage of AG16409 cells after XRCC1 KD at low FCS.

Additional file 5: Figure S5. Influence of ATF4 on siXRCC1 phenotype.

Additional file 6: Figure S6. Selective growth advantage of XRCC1 KD cells at 1% FCS depends on PERK activity.

Additional file 7: Figure S7. Validation of inhibitor activity.

Additional file 8: Figure S4. No influence of XRCC1 KD in siSp1 or IR treated cells grown at 5% FCS.

Additional file 9: Table S1. siRNA sequences used in this study.

Additional file 10: Table S2. List of primers used for qRT-PCR.

Additional file 11: Table S3. List of primary antibodies used.

Additional file 12: Table S4: All raw data for this study.

Acknowledgements

The authors thank the other members of the Institute of Veterinary Pharmacology and Toxicology for fruitful discussions and inputs to the project, Prof. M. Altmeyer and his group (University of Zürich) for access to and help with the Faxitron Cabinet X-ray system, the Zentrum für Klinische Forschung (University of Zürich) for access to their microscope system, and Prof. M. Kowalewski (University of Zürich) for access to his microscope.

Authors' contributions

EC designed, performed, and analysed most of the presented experiments with the help of LI, EB, CG, ZG, and EM. EM was responsible for the study design, supervision, funding, data analysis, and interpretation. EM wrote the first draft of the manuscript, and all authors contributed to the final manuscript. The authors read and approved the final manuscript.

Funding

This study was financially supported by the Heuberger Stiftung and the Fonds zur Förderung akademischer Nachwuchskräfte (Universität Zürich).

Availability of data and materials
All data generated or analysed during this study are included in the published article and its supplementary data files (Figs. 1, 2, 3, 4, 5 and Additional files 1, 2, 3, 4, 5, 6, 7, 8, 9, 10, 11, and 12).

Ethics approval and consent to participate
Not applicable.

Consent for publication
Not applicable.

Competing interests
The authors declare that they have no competing interests.

Received: 2 December 2019 Accepted: 16 March 2020
Published online: 30 March 2020

References

1. Maynard S, Fang EF, Scheibye-Knudsen M, Croteau DL, Bohr VA. DNA damage, DNA repair, aging, and neurodegeneration. Cold Spring Harb Perspect Med. 2015;5:a025130.
2. Markkanen E, Meyer U, Dianov GL. DNA damage and repair in schizophrenia and autism: implications for cancer comorbidity and beyond. Int J Mol Sci. 2016;17(6):856.
3. Jackson SP, Bartek J. The DNA-damage response in human biology and disease. Nature. 2009;461:1071–8.
4. van Loon B, Markkanen E, Hübscher U. Oxygen as a friend and enemy: how to combat the mutational potential of 8-oxo-guanine. DNA Repair (Amst). 2010;9:604–16.
5. Lindahl T. Instability and decay of the primary structure of DNA. Nature. 1993;362:709–15.
6. Dianov GL, Hübscher U. Mammalian base excision repair: the forgotten archangel. Nucleic Acids Res. 2013;41:3483–90.
7. Parsons JL, Tait PS, Finch D, Dianova II, Allinson SL, Dianov GL. CHIP-mediated degradation and DNA damage-dependent stabilization regulate base excision repair proteins. Mol Cell. 2008;29:477–87.
8. Parsons JL, Tait PS, Finch D, Dianova II, Edelmann MJ, Khoronenkova SV, et al. Ubiquitin ligase ARF-BP1/Mule modulates base excision repair. EMBO J Nature. 2009;28:3207–15.
9. Caldecott KW. XRCC1 protein; form and function. DNA Repair (Amst.). 2019; 8:102664.
10. Alexandrov LB, Nik-Zainal S, Wedge DC, Aparicio SAJR, Behjati S, Biankin AV, et al. Signatures of mutational processes in human cancer. Nature. 2013;500: 415–21.
11. Bartkova J, Horejsí Z, Koed K, Krämer A, Tort F, Zieger K, et al. DNA damage response as a candidate anti-cancer barrier in early human tumorigenesis. Nature. 2005;434:864–70.
12. Ma J, Setton J, Lee NY, Riaz N, Powell SN. The therapeutic significance of mutational signatures from DNA repair deficiency in cancer. Nat Commun. 2018;9: 1–12.
13. Wallace SS. Base excision repair: a critical player in many games. DNA Repair (Amst). 2014;19:14–26.
14. Roos WP, Thomas AD, Kaina B. DNA damage and the balance between survival and death in cancer biology. Nat Rev Cancer. 2015;16:20–33.
15. McNeill DR, Lin P-C, Miller MG, Pistell PJ, de Souza-Pinto NC, Fishbein KW, et al. XRCC1 haploinsufficiency in mice has little effect on aging, but adversely modifies exposure-dependent susceptibility. Nucleic Acids Res. 2011;39:7992–8004.
16. Lee Y, Katyal S, Li Y, El-Khamisy SF, Russell HR, Caldecott KW, et al. The genesis of cerebellar interneurons and the prevention of neural DNA damage require XRCC1. Nat Neurosci. 2009;12:973–80.
17. Dumitrache LC, Shimada M, Downing SM, Kwak YD, Li Y, Illuzzi JL, et al. Apurinic endonuclease-1 preserves neural genome integrity to maintain homeostasis and thermoregulation and prevent brain tumors. Proc Natl Acad Sci U S A. 2018;115:E12285–94.
18. Bajpai D, Banerjee A, Pathak S, Jain SK, Singh N. Decreased expression of DNA repair genes (XRCC1, ERCC1, ERCC2, and ERCC4) in squamous intraepithelial lesion and invasive squamous cell carcinoma of the cervix. Mol Cell Biochem. 2013;377:45–53.
19. Wang S, Wu X, Chen Y, Zhang J, Ding J, Zhou Y, et al. Prognostic and predictive role of JWA and XRCC1 expressions in gastric cancer. Clin Cancer Res. 2012;18:2987–96.
20. Kumar A, Pant MC, Singh HS, Khandelwal S. Reduced expression of DNA repair genes (XRCC1, XPD, and OGG1) in squamous cell carcinoma of head and neck in North India. Tumour Biol. 2012;33:111–9.
21. Mahjabeen I, Chen Z, Zhou X, Kayani MA. Decreased mRNA expression levels of base excision repair (BER) pathway genes is associated with enhanced Ki-67 expression in HNSCC. Med Oncol. 2012;29:3620–5.
22. Blomquist T, Crawford EL, Mullins D, Yoon Y, Hernandez D-A, Khuder S, et al. Pattern of antioxidant and DNA repair gene expression in normal airway epithelium associated with lung cancer diagnosis. Cancer Res. 2009;69:8629–35.
23. Sak SC, Harnden P, Johnston CF, Paul AB, Kiltie AE. APE1 and XRCC1 protein expression levels predict cancer-specific survival following radical radiotherapy in bladder cancer. Clin Cancer Res. 2005;11:6205–11.
24. Markkanen E. Not breathing is not an option: how to deal with oxidative DNA damage. DNA Repair (Amst). 2017;59:82–105.
25. Poletto M, Legrand AJ, Fletcher SC, Dianov GL. p53 coordinates base excision repair to prevent genomic instability. Nucleic Acids Res. 2016;44: 3165–75.
26. Legrand AJ, Poletto M, Pankova D, Clementi E, Moore J, Castro-Giner F, et al. Persistent DNA strand breaks induce a CAF-like phenotype in normal fibroblasts. Oncotarget. 2018;9:13666–81.
27. Fletcher SC, Grou CP, Legrand AJ, Chen X, Soderstrom K, Poletto M, et al. Sp1 phosphorylation by ATM downregulates BER and promotes cell elimination in response to persistent DNA damage. Nucleic Acids Res. 2018; 46: 1834–46.
28. Markkanen E, Fischer R, Ledentcova M, Kessler BM, Dianov GL. Cells deficient in base-excision repair reveal cancer hallmarks originating from adjustments to genetic instability. Nucleic Acids Res. 2015;43:3667–79.
29. Harding HP, Zhang Y, Zeng H, Novoa I, Lu PD, Calfon M, et al. An integrated stress response regulates amino acid metabolism and resistance to oxidative stress. Mol Cell. 2003;11:619–33.
30. Singleton DC, Harris AL. Targeting the ATF4 pathway in cancer therapy. Expert Opin Ther Targets. 2012;16:1189–202.
31. Wortel IMN, van der Meer LT, Kilberg MS, van Leeuwen FN. Surviving stress: modulation of ATF4-mediated stress responses in normal and malignant cells. Trends Endocrinol Metab. 2017;28:794–806.
32. Pakos Zebrucka K, Koryga I, Mnich K, Ljujic M, Samali A, Gorman AM. The integrated stress response. EMBO Rep. 2016;17:1374–95.
33. Axten JM, Medina JR, Feng Y, Shu A, Romeril SP, Grant SW, et al. Discovery of 7-methyl-5-(1-[[3-(trifluoromethyl)phenyl]acetyl]-2,3-dihydro-1 H-indol-5-yl)-7 H-pyrrolo[2,3- d]pyrimidin-4-amine (GSK2606414), a potent and selective first-in-class inhibitor of protein kinase R (PKR)-like endoplasmic reticulum kinase (PERK). J Med Chem. 2012;55:7193–207.
34. Orlando G, Khoronenkova SV, Dianova II, Parsons JL, Dianov GL. ARF induction in response to DNA strand breaks is regulated by PARP1. Nucleic Acids Res. 2014;42:2320–29.
35. Khoronenkova SV, Dianov GL. ATM prevents DSB formation by coordinating SSB repair and cell cycle progression. Proc Natl Acad Sci U S A. 2015;112: 3997–4002.
36. Plumb MA, Smith GCM, Cunniffe SMT, Jackson SP, O'Neill P. DNA-PK activation by ionizing radiation-induced DNA single-strand breaks. Int J Radiat Biol. 2009;75:553–61.
37. Chaudhuri AR, Nussenzweig A. The multifaceted roles of PARP1 in DNA repair and chromatin remodelling. Nat. Rev. Mol. Cell Biol. Nat Publ Group; 2017;18:610–621.
38. Shiloh Y, Ziv Y. The ATM protein kinase: regulating the cellular response togenotoxic stress, and more. Nature Publishing Group. 2013;14:1–14.
39. Brem R, Hall J. XRCC1 is required for DNA single-strand break repair in human cells. Nucleic Acids Res. 2005;33:2512–20.
40. Bauer M, Goldstein M, Christmann M, Becker H, Heylmann D, Kaina B. Human monocytes are severely impaired in base and DNA double-strand break repair that renders them vulnerable to oxidative stress. Proc Natl Acad Sci U S A. 2011;108:21105–10.
41. Narciso L, Fortini P, Pajalunga D, Franchitto A, Liu P, Degan P, et al. Terminally differentiated muscle cells are defective in base excision DNA repair and hypersensitive to oxygen injury. Proc Natl Acad Sci U S A. 2007; 104:17010–5.
42. Ponath V, Heylmann D, Haak T, Woods K, Becker H, Kaina B. Compromised DNA repair and signalling in human granulocytes. J Innate Immun. 2018;11: 74–85.

43. Chan N, Ali M, McCallum GP, Kumareswaran R, Koritzinsky M, Wouters BG, et al. Hypoxia provokes base excision repair changes and a repair-deficient, mutator phenotype in colorectal cancer cells. Mol Cancer Res. 2014;12:1407–15.
44. Smith TB, Dun MD, Smith ND, Curry BJ, Connaughton HS, Aitken RJ. The presence of a truncated base excision repair pathway in human spermatozoa that is mediated by OGG1. J Cell Sci. 2013;126:1488–97.
45. Briegert M, Kaina B. Human monocytes, but not dendritic cells derived from them, are defective in base excision repair and hypersensitive to methylating agents. Cancer Res. 2007;67:26–31.
46. Bauer M, Goldstein M, Heylmann D, Kaina B. Human monocytes undergo excessive apoptosis following temozolomide activating the ATM/ATR pathway while dendritic cells and macrophages are resistant. Jacobs R, editor. PLoS One. 2012;7:e39956.
47. Wang E. Senescent human fibroblasts resist programmed cell death, and failure to suppress bcl2 is involved. Cancer Res. 1995;55:2284–92.
48. Hanahan D, Coussens LM. Accessories to the crime: functions of cells recruited to the tumor microenvironment. Cancer Cell. 2012;21:309–22.
49. Madar S, Goldstein I, Rotter V. "Cancer associated fibroblasts"—more than meets the eye. Trends Mol Med. 2013;19:447–53.
50. Costa A, Scholer-Dahirel A, Mechta-Grigoriou F. The role of reactive oxygen species and metabolism on cancer cells and their microenvironment. Semin Cancer Biol. 2014;25:23–32.
51. Tigges J, Krutmann J, Fritsche E, Haendeler J, Schaal H, Fischer JW, et al. Mechanisms of ageing and development. Mechanisms Ageing Dev. 2014;138:26–44.
52. Lyssiotis CA, Kimmelman AC. Metabolic interactions in the tumor microenvironment. Trends Cell Biol. 2017;27:863–75.
53. Guan B-J, van Hoef V, Jobava R, Elroy-Stein O, Valasek LS, Cargnello M, et al. A unique ISR program determines cellular responses to chronic stress. Mol Cell. 2017;68:885–6.
54. Lee HW, Park YM, Lee SJ, et al. Alpha-smooth muscle actin (ACTA2) is required for metastatic potential of human lung adenocarcinoma. Clin Cancer Res. 2013;19:5879–89. https://doi.org/10.1158/1078-0432.CCR-13-1181.
55. Gyori BM, Venkatachalam G, Thiagarajan PS, Hsu D, Clement M-V. Redox biology. Redox Biol. 2014;2:457–65.
56. Wojewódzka M, Buraczewska I, Kruszewski M. A modified neutral comet assay: elimination of lysis at high temperature and validation of the assay with anti-single-stranded DNA antibody. Mutat Res. 2002;518:9–20.

Publisher's Note

6.2 Investigating possible mechanisms underlying the XRCC1 KD mediated survival advantage in TIG-1 fibroblasts

Considering the findings presented in the paper shown in chapter 6.1 of this thesis, we next asked ourselves how an XRCC1 KD and the following activation of the ISR could confer the cells with a survival advantage under nutrient restricted conditions. In other words, what is the mechanism that drives the increased survival of XRCC1 KD cells under nutrient restriction.

6.2.1 XRCC1 KD does not increase the autophagic activity of TIG-1 cells

Our hypothesis was that XRCC1 KD followed by an upregulation of ATF4 could increase the autophagic activity in the fibroblasts, which in turn could provide self-sufficiency with respect to nutrients in a way that the cells would depend less on exogenous nutrient supply. This hypothesis was supported by the fact that ATF4 was already known to play a role in regulation of autophagy [26,33].

To investigate whether XRCC1 KD cells have a higher autophagic activity than control cells, we transfected TIG-1 cells with siCon or siXRCC1 and treated them with chloroquine, a known autophagy inhibitor [32,57]. Two hours after addition of the inhibitor, we collected the cells for protein analysis (see Figure 1 for a scheme of the experimental setup). To analyse the autophagic flux we checked the known markers for autophagy, p62 and LC3, by Western blot. LC3 is present in cells in two different forms, LC3-I and LC3-II. LC3-II migrates slightly below LC3-I in a Western blot (Figure 5A). When autophagy is active, both LC3-II and p62 are degraded, which reduces their protein levels. When such cells are treated with the autophagy inhibitor chloroquine, an increase in LC3-II or p62 in comparison to control treated cells is indicative of active autophagy, as the two proteins are not degraded anymore through the autophagic pathway (Figure 5A, compare lanes + and - chloroquine). Under conditions of increased autophagy, for example during nutrient starvation, chloroquine treatment will cause a stronger surge in the levels of LC3-II and p62 (Figure 5A). Thus, the relative increase of LC3-II and p62 levels after chloroquine treatment with respect to control treated cells is indicative of active autophagic flux in these cells [31,58].

Using this setup, analysis of protein levels of siCon cells treated with chloroquine revealed a clear increase in LC3-II compared to control-treated cells (Figure 5B). This suggested that the chloroquine treatment was indeed able to block autophagic depletion of LC3-II and that a basal level of autophagy was active in siCon cells. A very similar increase in LC3-II levels could be observed upon inhibitor treatment of siXRCC1 cells (Figure 5B). Indeed, quantification of LC3-I and LC3-II levels clearly showed that there was no difference in the increase of LC3-II upon chloroquine treatment between siCon and siXRCC1 treated cells (Figure 5C). These results suggested that there was a basal level of autophagy ongoing in both siCon and siXRCC1 cells under the conditions used, but the level of autophagy was comparable between these two conditions. Similarly, also the levels of the second autophagy marker p62 increased in the siCon cells upon chloroquine treatment (Figure 5B and D), further supporting the results obtained by LC3-II. Interestingly however, the XRCC1 KD cells displayed a significant decrease in p62 protein level compared to siCon cells under basal, non-chloroquine treated conditions (Figure 5B and D). Surprisingly, these low levels of p62 could not be rescued by inhibitor treatment (Figure 5B and D). Hence, the low levels of p62 observed after siXRCC1 treatment were not caused by increased autophagy. Taken together, these results further underlined the notion that there was no difference in autophagic activity between control cells and cells depleted of XRCC1.

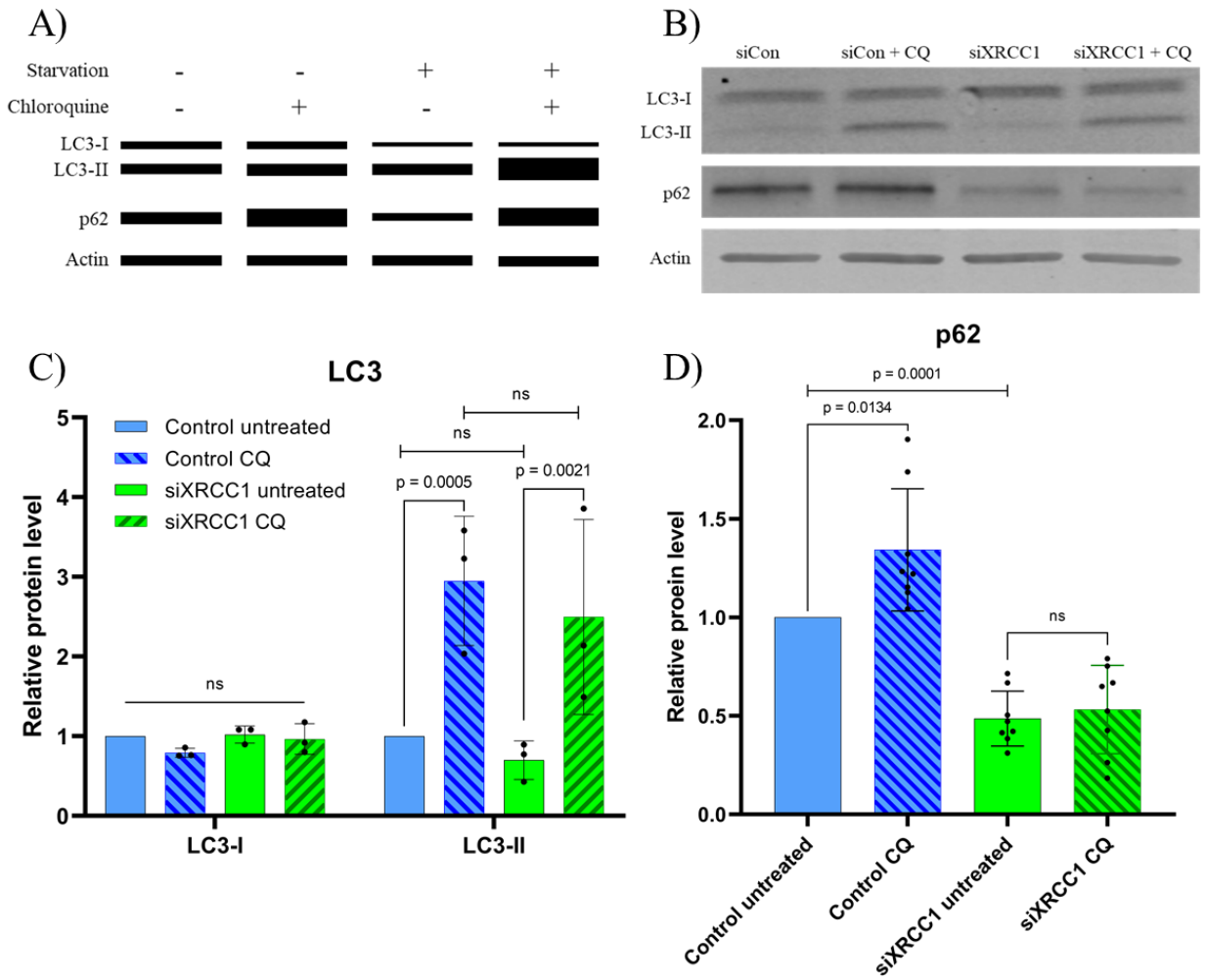

Figure 5: Autophagic flux is not increased in siXRCC1 cells. (A) Schematic example for the analysis of the autophagic flux by Western blot. Autophagy induction by nutrient starvation decreases LC3-II and p62 protein levels due to their degradation. When autophagy is inhibited by chloroquine, an increase in LC3-II and p62 can be seen, because they are not degraded anymore. The autophagic flux is assessed by the relative increase of LC3-II and p62 protein levels after inhibitor treatment compared to basal conditions. (B) Representative Western blot of the LC3 and p62 levels in siCon and siXRCC1 cells treated with dH_2O (control) or chloroquine (CQ), respectively. Actin was used as loading control. (C) Quantification of LC3-I and LC3-II protein levels as seen in B). Values are presented as mean ±SD normalised to actin as loading control from three independent experiments, with the control treatment set to 1. The dots represent all individual values of different experiments. (D) Quantification of p62 protein levels as seen in B). Values are presented as mean ±SD normalised to actin as loading control from eight independent experiments with the control treatment set to 1. The dots represent all individual values of different experiments.

6.2.2 Analysing the connection between XRCC1 depletion and a decrease in p62 in TIG-1 cells

Having found a decrease of p62 protein upon XRCC1 KD that was independent of autophagy (Figure 5B and D), and the known involvement of a loss of p62 expression in CAF biology, we next wanted to investigate this connection between XRCC1 and p62 more closely.

6.2.2.1 p62 mRNA level in TIG-1 cells is not influenced by XRCC1 KD

The decrease in p62 protein level mediated by XRCC1 KD could either be due to a transcriptional or post-transcriptional decrease of p62. To differentiate between these scenarios, we analysed p62 mRNA levels after siCon and siXRCC1 treatment by RT-qPCR. For this, we extracted mRNA from TIG-1 fibroblasts transfected with siCon or two different siRNA sequences against XRCC1 (designated siXRCC1-1 and siXRCC1-3). Both siRNA sequences for XRCC1 were efficient in down-regulating mRNA levels of XRCC1 (Figure 6), achieving a downregulation of XRCC1 of about 70 to 90%. Using this setup, we could not detect any significant difference in p62 mRNA

levels between siCon and siXRCC1 KD cells (Figure 6). These results were confirmed in several independent repetitions of the experiment (n = 4 for siXRCC1-1 and n = 2 for siXRCC1-3). Hence, the decrease in p62 protein levels upon XRCC1 KD was not due to a transcriptional suppression of p62 mRNA.

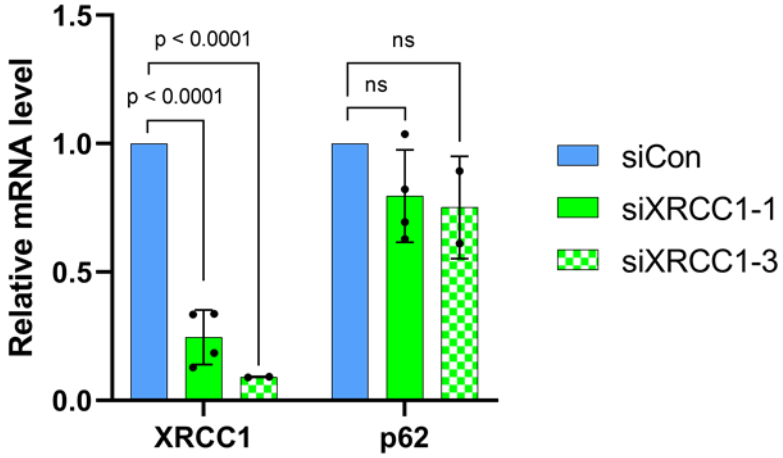

Figure 6: mRNA levels of p62 are not influenced by XRCC1 KD. mRNA levels of indicated genes in siCon and siXRCC1 fibroblasts analysed by RT-qPCR. Values were normalised to GAPDH and B2M with the siCon cells set to 1. Data are presented as mean ±SD and the dots represent the individual values from independent repetitions of the experiment (n = 4 for siXRCC1-1 and n = 2 for siXRCC1-3).

6.2.2.2 The decrease in p62 protein levels in XRCC1 KD cells depends on signalling by ATM

As the decrease in p62 protein levels after XRCC1 KD was not caused by a decrease in mRNA levels, we next decided to investigate the post-transcriptional regulation of p62. In the paper outlined in chapter 6.1 (Figure 4), we showed that XRCC1 KD activated the kinase ATM through generation of persistent SSBs, which then in turn triggered the activation of the protein kinase PERK. Subsequently, PERK phosphorylated eIF2α, which lead to a global decrease in translation and at the same time to a preferential increase in translation of a handful of specific stress-response proteins, such as ATF4 [26,59,60]. This led us to hypothesise that the decrease of p62 protein could be due to the global suppression in translation brought about by ATM-mediated phosphorylation of eIF2α.

To test this, we assessed the effect of ATM inhibition in siCon and siXRCC1 treated cells on p62 protein levels by Western blot (see Figure 2 for a scheme of the experiment and Figure 7C for treatment validation). As expected, siXRCC1 treated cells showed a marked decrease in p62 levels compared to siCon cells (Figure 7A, B). Interestingly, addition of an ATM inhibitor was able to completely rescue p62 levels in XRCC1 KD cells (Figure 7A, B). ATM inhibition also led to a further increase of p62 in control cells (Figure 7A and B), suggesting that basal activity of ATM constantly suppresses p62 levels also under normal conditions. Thus, the decrease in p62 protein levels after XRCC1 KD seemd to be mediated through signalling of DNA damage by ATM.

To investigate, whether the decrease in p62 also depended on PERK, we investigated the effect of PERK depletion on p62 protein levels using siRNA against PERK in XRCC1 KD cells. To do so, we transfected TIG-1 cells with either siCon, siXRCC1, siPERK or a combination of siXRCC1 and siPERK (see Figure 3 for a scheme of the experiment and Figure 7F for treatment validation). Surprisingly however, PERK KD alone already decreased the levels of p62 to an even greater extent as siXRCC1 treatment (Figure 7D and E). Similarly, the combined siXRCC1 and siPERK treated cells showed low levels of p62 (Figure 7D and E). Hence, PERK did not seem to play a role in the post-transcriptional decrease of p62 upon XRCC1 KD.

Finally, to understand whether ATF4 as a downstream effector of the integrated stress response was involved in the suppression of p62 protein levels upon XRCC1 KD, we assessed the effect of ATF4 depletion using siRNA in XRCC1 KD cells (see Figure 3 for a scheme of the experiment

and Figure 7I for treatment validation). Similarly to PERK, also ATF4 KD alone already led to reduced levels of p62, and was not able to rescue p62 protein levels in cells depleted of XRCC1 (Figure 7G and H).
Taken together, these experiments showed that signalling of DNA damage by ATM was involved in the decrease of p62 protein levels, but that the suppression of p62 was independent of signalling through PERK or ATF4.

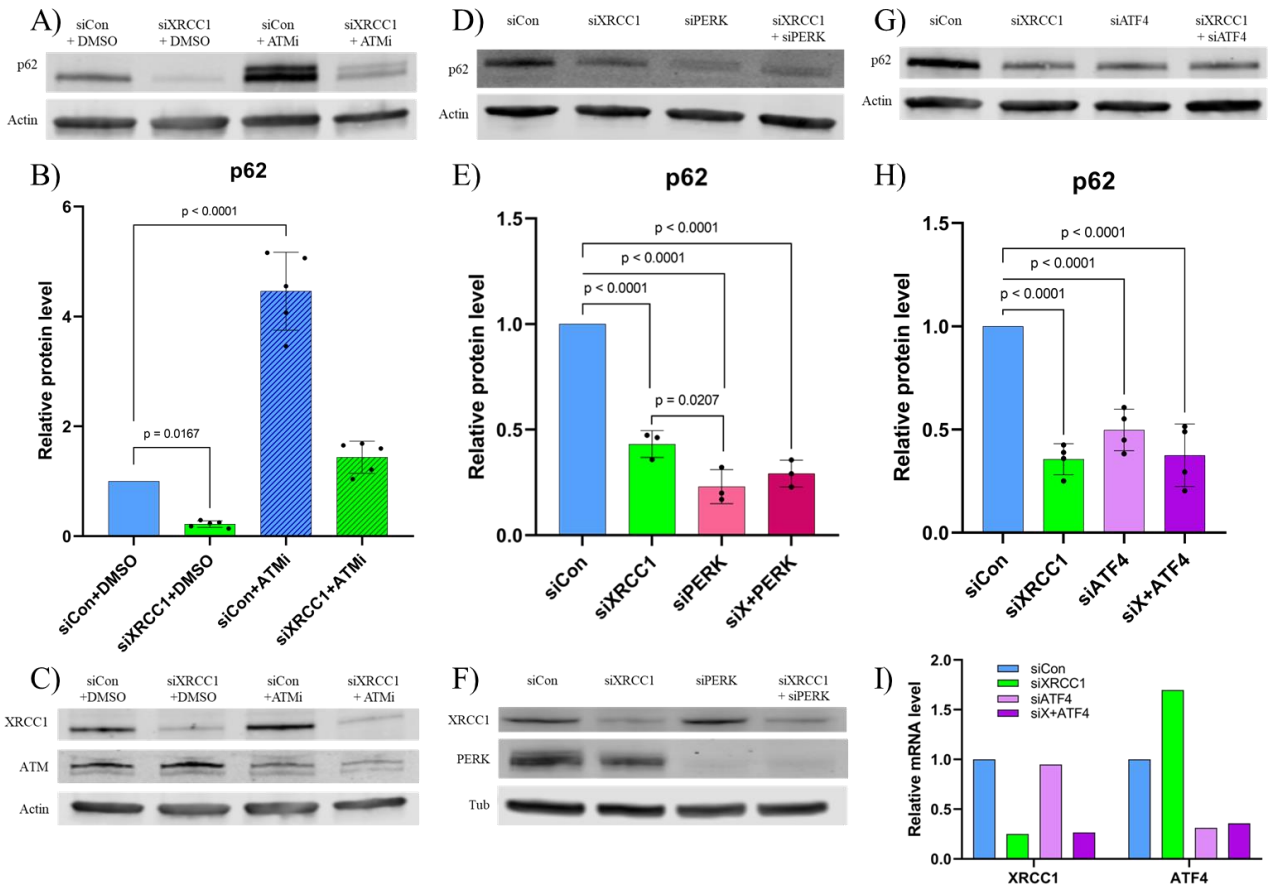

Figure 7: Analysis of p62 protein level in TIG-1 cells (A) Western blot analysis of p62 in XRCC1 KD and control cells treated with ATM inhibitor or an equivalent amount of DMSO. Actin was used as loading control (B) Quantification of p62 protein level as seen in A). Values are mean ±SD normalised to actin as loading control. Each dot represents an individual value of an experiment, from five independent experiments. (C) Western blot analysis of XRCC1 and ATM protein in XRCC1 KD and control cells treated with ATM inhibitor or an equivalent amount of DMSO. Actin was used as loading control (D) Western blot analysis of p62 in TIG-1 fibroblasts transfected with siCon, siXRCC1, siPERK and a combination of siXRCC1 and siPERK. Actin was used as a loading control. (E) Quantification of p62 protein level as seen in D) Values are mean ±SD normalised to actin as loading control. Each dot represents an individual value of an experiment, from three independent experiments. (F) Western blot analysis of XRCC1 and PERK protein in TIG-1 fibroblasts transfected with siCon, siXRCC1, siPERK and a combination of siXRCC1 and siPERK. Tubulin was used as a loading control. (G) Western blot analysis of p62 in TIG-1 fibroblasts transfected with siCon, siXRCC1, siATF4 and a combination of siXRCC1 and siATF4. Actin was used as a loading control. (H) Quantification of p62 protein level as seen in G) Values are mean ±SD normalised to actin as loading control. Each dot represents an individual value of an experiment, from four independent experiments. (I) RT-qPCR quantification of XRCC1 and ATF4 mRNA in TIG-1 fibroblasts transfected with siCon, siXRCC1, siATF4 and a combination of siXRCC1 and siATF4. Values were normalised to GAPDH and B2M with the siCon cells set to 1.

6.2.2.3 The induction of direct DNA damage through H_2O_2 causes a decrease in p62 likewise

Since our data suggested the decrease in p62 protein levels in XRCC1 KD cells to be connected to DNA damage signalling through ATM, we wanted to investigate whether the same effect could also be achieved by direct induction of DNA damage.
For this, TIG-1 fibroblasts were chronically exposed to different low doses of hydrogen peroxide for a period of 72h and collected for protein analysis. Indeed, cells treated with H2O2 showed a significant, dose-dependent decrease in p62 protein levels compared to control (Figure 8A and B).

From this we conclude that DNA damage signalling really was involved in inducing a decrease of p62 protein levels.

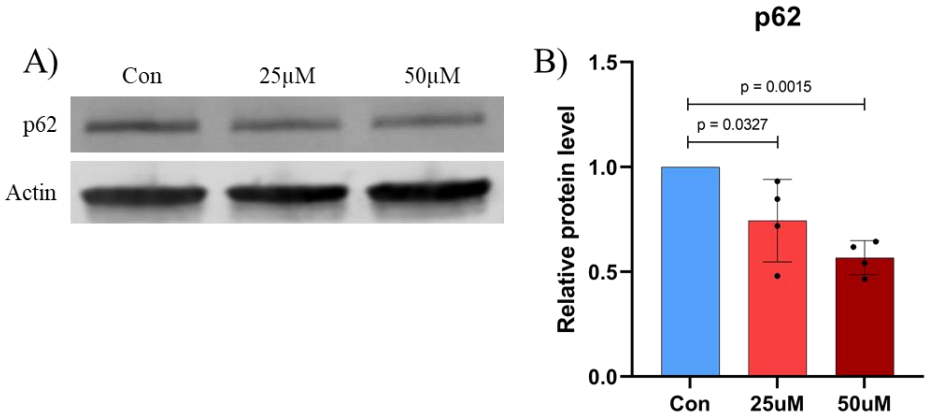

Figure 8: p62 protein level in TIG-1 cells treated with H_2O_2 (A) Western blot analysis of p62 in TIG-1 fibroblasts treated with H_2O_2 or corresponding amount of dH_2O. Actin was used as loading control. (B) Quantification of p62 protein levels as seen in A9. Values are mean ±SD normalised to actin as loading control, the dots represent all individual values of different experiments from four independent experiments.

6.2.3 Metabolic reprograming through XRCC1 KD does not depend on ASNS

The initial question of this part of the project was to investigate the mechanism behind the survival advantage of TIG-1 fibroblasts depleted of XRCC1. Since we found XRCC1 KD to be able to decrease p62 protein levels, we wanted to investigate whether this could play a role in the increased survival of these cells. In literature, p62 KD in cells was reported to promote cell survival under glutamine-deprived conditions through an upregulation of ASNS [47]. To test whether the same mechanism applied to our XRCC1 KD fibroblasts, we transfected TIG-1 cells with siCon, siXRCC1, two different siRNA sequences for ASNS and a combination of each of these sequences with siXRCC1 and cultured them in medium containing different amounts of FCS (see Figure 4 for a scheme of the experiment).

6.2.3.1 Checking KD efficiency of two different siRNA targeting ASNS

Since ASNS KD has not been performed before in our lab we first tested the efficiency of two different siRNAs. In addition, we investigated the effect of XRCC1 KD on ASNS on transcriptional level. For this we extracted mRNA from cells collected three days after transfection and performed RT-qPCR. Both, siASNS-1 and siASNS-2, reach an appropriate downregulation of ASNS and the mRNA level was not influenced by the co-KD with XRCC1 (Figure 9). Interestingly, an upregulation of XRCC1 could be seen in the ASNS KD cells and, vice versa, XRCC1 KD induced an upregulation of ASNS. The reason for such compensatory upregulation remained unclear, but it is tempting to speculate that the two genes might be linked through some kind of feedback loop.

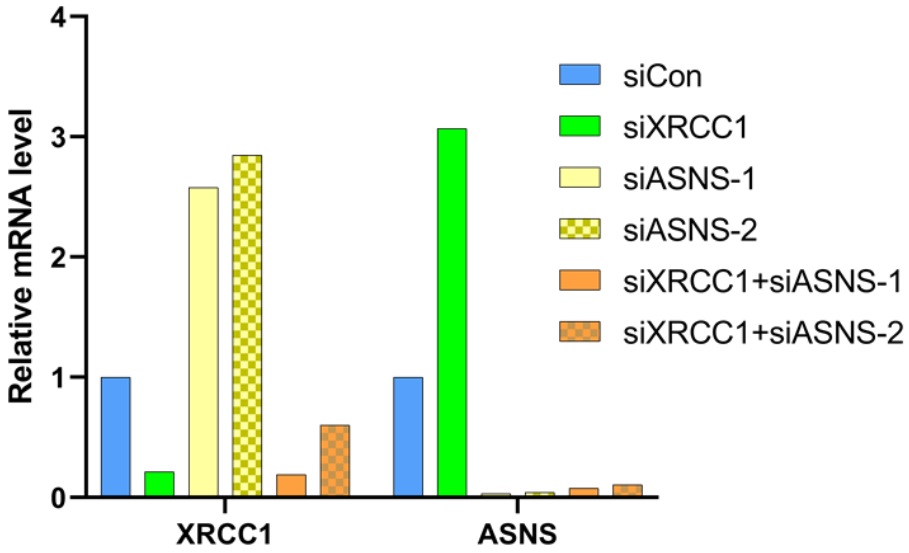

Figure 9: Validation of KD by siRNA. RT-qPCR quantification of XRCC1 and ASNS mRNA level in TIG-1 fibroblasts transfected with siRNA as indicated. Values were normalised to GAPDH and B2M with the siCon cells set to 1.

6.2.3.2 The survival advantage of XRCC1 KD cells is independent of ASNS

Once the downregulation was validated and an upregulation of ASNS following XRCC1 KD was shown, we investigated the effect of knocking down ASNS alone or in combination with XRCC1 in view of cell survival under nutrient restricted conditions. We exposed the transfected cells to culture medium containing different amounts of FCS and took pictures of the cells 72h after the KD to analyse cell density and morphology. When cells were grown in medium containing sufficient amount of FCS, no clear differences in cell number or morphology could be observed (Figure 10). As expected, in medium containing just 1% FCS XRCC1 KD cells clearly displayed an increased cell number compared to the control (Figure 11A and B). However, this increase in cell number was still visible when XRCC1 KD was combined with either of the siRNAs against ASNS (Figure 11E and F). The ASNS KD alone seemed to have no influence on the cell survival, as they looked virtually indistinguishable from control (Figure 11C and D).
In conclusion, these findings suggest that the survival advantage of XRCC1 KD cells under nutrient restriction did not depend on ASNS.

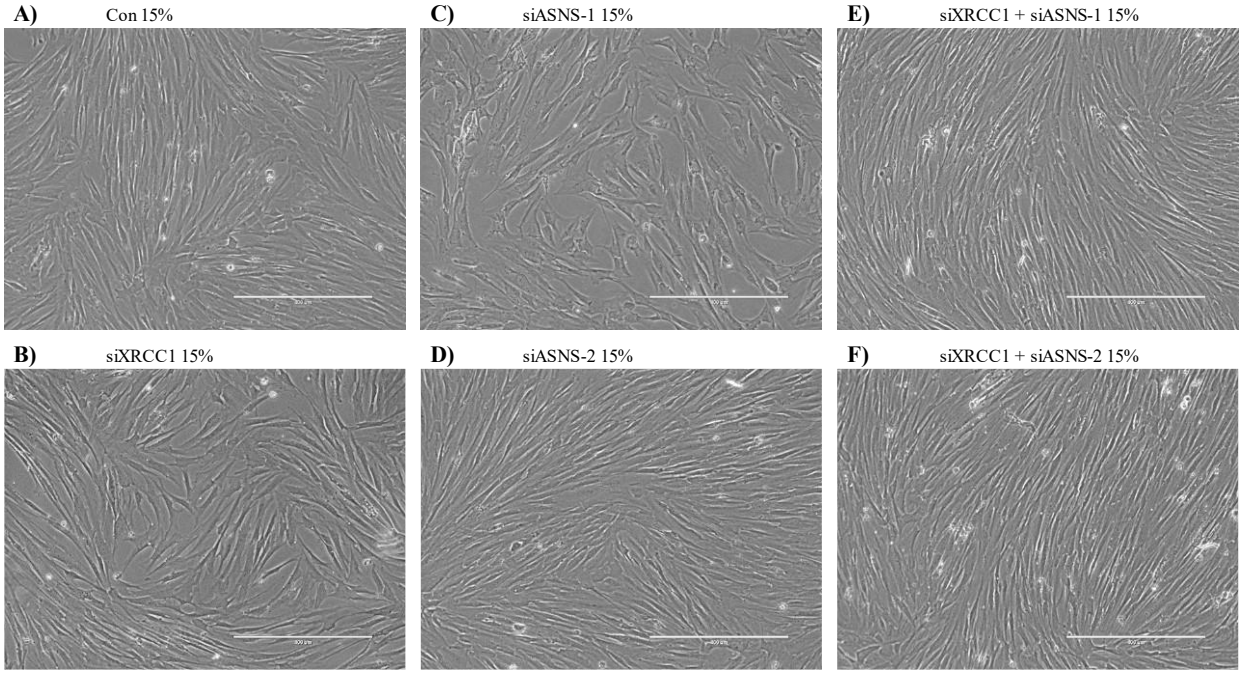

Figure 10: No difference in growth of TIG-1 cells at 15% FCS. Representative phase-contrast images of TIG-1 human fibroblasts from one representative experiment taken on the third day upon transfection with siRNAs as indicated, started with the same number of cells in each condition and split to DMEM medium containing 15% of FCS 24h after transfection. The shown field is randomly chosen on each plate, from one out of two independent experiments.

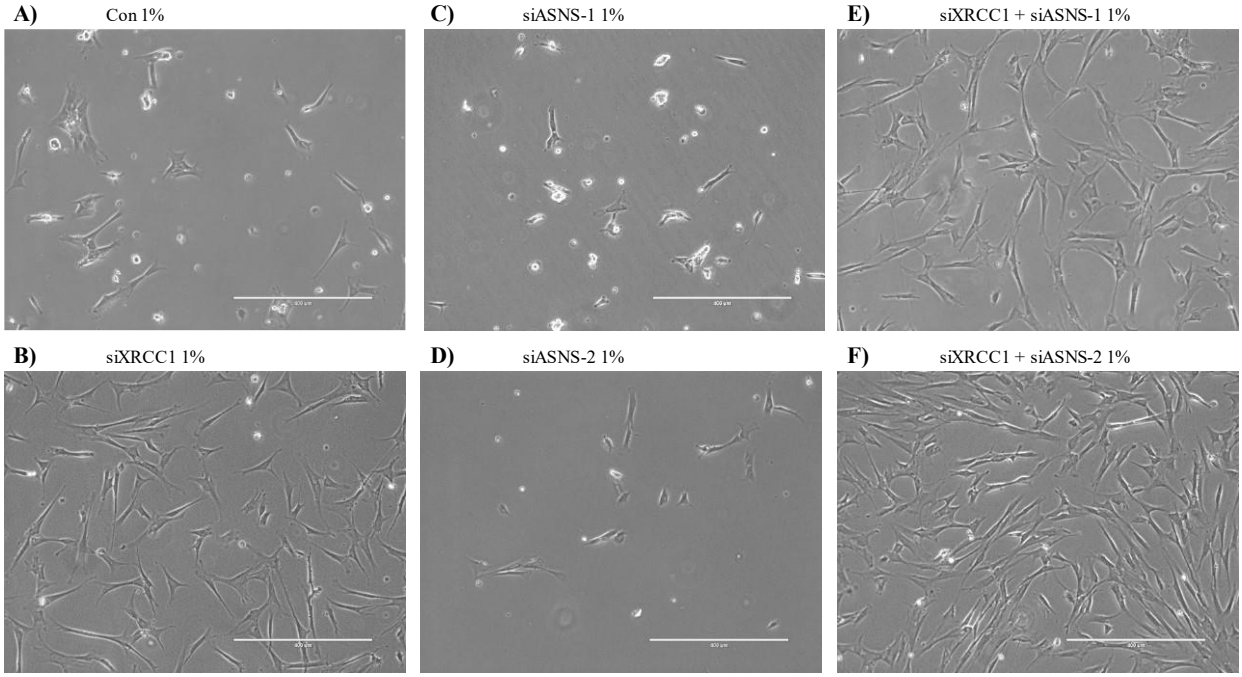

Figure 11: Growth advantage of XRCC1 KD cells is not influenced by siASNS at 1% FCS. Representative phase-contrast images of TIG-1 human fibroblasts from one representative experiment taken on the third day upon transfection with siRNAs as indicated, started with the same number of cells in each condition and split to DMEM medium containing 1% of FCS 24h after transfection. The shown field is randomly chosen on each plate, from one out of two independent experiments.

7 Discussion

Cancer is a big burden for today's global health care system. Despite much ongoing research to develop new treatments and diagnostic approaches, about 1 in 6 deaths worldwide is due to cancer [1]. Recent findings have shown that not only the cancer cells themselves are relevant for the disease, but also the surrounding CAS plays a pivotal role in cancer biology. Hence, targeting CAS is viewed as a promising approach to find new therapies [3,4,7]. One prominent cellular component within CAS are the CAFs. CAFs are able to strongly support tumour growth and metastasis, therefore acting as a major factor in determining the tumour outcome for patients [8].
It has been shown that CAF formation can be induced by inflammatory cytokines, such as TGF β and/or ROS *in vitro* [23,24]. Recently, our group found that exposure of fibroblasts to these agents promotes a decrease in XRCC1, which caused persistent DNA damage, due to a lack of BER capacity. This in turn led to the transformation of these fibroblasts into CAFs. Accordingly, this CAF-reprogramming of fibroblasts could also be observed by just knocking-down XRCC1, suggesting persistent DNA damage as the molecular driver in CAF activation. The reprogramming depended at least partly on the integrative stress response through ATF4 upregulation, which seemed to shift cellular metabolism towards an increase in nutritional self-sufficiency [13,25]. But the reason for and the consequences of this metabolic reprogramming were unclear.

7.1 XRCC1 KD imparts TIG-1 fibroblasts with a survival advantage under nutrient restriction mediated through ATF4

Based on the data outlined above, we hypothesised that XRCC1 KD could impart cells with an advantage to survive better in conditions of nutrient restriction. Following this hypothesis, we confirmed that XRCC1 KD cells really had a survival advantage over control cells (Chapter 6.1 Figure 1D and E). Moreover, fibroblasts with a combined KD of ATF4 and XRCC1 did not show the increased survival anymore. This suggested that the increased survival depended on ATF4 (Chapter 6.1 Figure 2D and E). We also confirmed that the KD efficiency of the siRNAs was not influenced by the different FCS concentrations by assessing mRNA levels of direct targets and several downstream targets (Chapter 6.1 Figure 2F).
The finding that fibroblasts with an accumulation of persistent DNA damage due to a deficiency in BER capacity could survive better under nutrient restricted conditions was very promising. Previously it was shown that chronic exposure to two agents known to induce CAF activation, namely ROS and pro-inflammatory cytokines, lead to persistent DNA damage that was caused by a BER decline through downregulation of XRCC1 [25]. Based on this it was assumed that CAF activation should also be triggered by a direct KD of XRCC1 without exposure to DNA damaging agents. Indeed, downregulation of XRCC1 alone was enough to trigger the transformation of normal fibroblasts into CAFs, suggesting persistent DNA damage is crucial for CAF activation [25]. But still these findings did not explain why cells should lower their BER capacity under stressful conditions. One explanation that was put forward was, that these cells could potentially be better eliminated by the immune system or be 'self-removed' through apoptotic mechanisms [61]. However, fibroblasts are cells that are highly resistant to apoptosis, instead they rather undergo senescence so they can maintain the structure of the extracellular matrix [62]. If they would easily undergo apoptosis when damaged, this might have devastating effects on tissue integrity.
Moreover, our lab uncovered a wide-ranging metabolic reprogramming in fibroblasts with a BER deficiency mediated through XRCC1 KD (unpublished data). We assumed that these changes enables the cells to grow more independent of nutrient supply, as they increase their self-sufficiency. As the findings in our paper (Chapter 6.1) showed that fibroblasts with a BER deficiency grew better under nutrient restricted conditions due to an ATF4 mediated reprogramming this further supported the functionality of these metabolic changes. Through this reprogramming, the fibroblasts might still be able to fulfil their role to provide structure and stability even under stressful circumstances [63].

Implications of these results for CAF biology are quite interesting. CAFs are cells located in next proximity to rapidly growing cancer cells. Cancer cells are known to be highly proliferative and therefore also to display a huge demand for nutrients. Accordingly, they reprogram their metabolism to enhance nutrient uptake as to sustain their growth and survival [42]. In addition, it was also shown that they influenced the surrounding stroma in a way to increase nutrient delivery towards the cancer cells [4,64]. Specifically, CAFs rewired their metabolism to recycle the metabolic waste of cancer cells and in turn secreted it again to feed the tumour [46,65,66]. Thus, it is thought that cancer cells use up most of the available nutrients and thereby leave the surrounding CAFs in a nutrient starved environment[47]. Our findings implicated, that the decline in BER capacity found in CAFs increased their nutritional self-sufficiency as a physiological response to ensure their survival in the stressed environment next to cancer cells.
The exact mechanisms and the driving forces for this survival advantage under nutrient restriction remained still unclear. However, a closer investigation of this phenomenon would be important, as the mechanism underlying the increased survival could potentially be used as a target for therapeutic interventions to remove CAFs. Preventing CAFs from surviving in the stressed tumour environment would also stop them from supporting cancer growth, which might well improve the success of currently used cancer-cell targeted treatments.

7.2 Autophagy is not involved in the XRCC1 KD mediated survival advantage under nutrient restricted conditions

Having established an unexpected connection between BER capacity, persistent DNA damage and reprogramming of the cellular metabolism through the integrated stress response factor ATF4, we next wanted to investigate possible mechanisms behind the survival advantage of XRCC1 KD cells under nutrient restriction. ATF4 is known to be involved in the regulation of autophagy in response to several stresses [33,67]. An autophagy gene transcriptional program is activated through the eIF2α/ATF4 pathway where ATF4 regulates the transcription of a large number of genes involved in the formation, elongation and function of the autophagosome [33]. Autophagy is a cellular process that involves the lysosomal degradation of cytoplasmic constituents such as proteins and organelles [33,68,69]. It is known that the degradation products resulting from autophagy can be recycled to provide sources of energy or base material for the synthesis of new macromolecules [70]. This led us to hypothesise that an increase in autophagy could enhance cellular self-sufficiency. By assessing the autophagic flux in control cells and cells depleted of XRCC1 we were able to show that there was no significant difference in autophagy (Figure 5B and C). This suggested that autophagy is not relevant for the XRCC1 mediated survival advantage, and that another, yet unidentified mechanism imparts cells depleted of XRCC1 with a survival advantage under nutrient restriction.

7.3 An unexpected connection between XRCC1 KD and decreased expression of p62

During the experiments for autophagy assessment, we observed a striking loss of p62 protein in XRCC1 KD cells which could not be rescued by inhibiting autophagy (Figure 5). Due to this missing response to autophagy inhibition, we assumed that the loss of p62 was independent of degradation through autophagy and instead mediated through another mechanism. This finding was interesting as p62 was already known to be involved in several processes such as inflammation, cell death, survival, and metabolic reprogramming, as well as in CAF activation [42,44].
An analysis of p62 mRNA levels revealed that the loss of p62 was depended on a post-transcriptional mechanism, since we could not see significant differences in p62 mRNA levels in XRCC1 KD cells compared to control (Figure 6). As we knew from the data presented in our paper (Chapter 6.1) SSBs generated through XRCC1 KD led to ATM-mediated activation of the PERK-peIF2α-ATF4 pathway. It is a pathway that is known to be part of the ISR and is activated upon ER stress [60,71]. Phosphorylation of eiF2α results in a global reduction of protein synthesis and at the same time to preferential stimulation of translation of specific mRNAs [26,59,60]. Therefore, we

hypothesised that p62 protein in XRCC1 KD cells could be lower due to the global decrease in translation. To understand this, we designed experiments where we sequentially suppressed the players involved in the pathway in addition to XRCC1 KD. By inhibiting ATM in XRCC1 KD TIG-1 cells we could show a connection of p62 and ATM, as the loss of p62 could be rescued to a level that was comparable with the one found in untreated control cells (Figure 7A, B and C). However, this rescue could not be achieved by downregulation of PERK or ATF4 together with XRCC1 (Figure 7D – I). Based on these findings we assumed that another mechanism than the phosphorylation of eIF2α with following suppression of translation must have been relevant for the loss of p62 in cells depleted of XRCC1. However, we could not definitely exclude the involvement of peIF2α. Since for a lack of time just the involvement of PERK and ATF4 could be excluded, it might still be possible that phosphorylation of eIF2α could be triggered through another mechanism and in turn inhibited global translation, including the one of p62. Four serine/threonine eIF2α kinases are known to be able to catalyse the phosphorylation of eiF2α, namely PKR-like ER kinase (PERK), double-stranded RNA-dependent protein kinase (PKR), heme-regulated eIF2α kinase (HRI), and general control non-derepressible 2 (GCN2) [26]. In our paper (chapter 6.1) we could show that the kinase GCN2 was unable to rescue XRCC1 KD-mediated upregulation of ATF4 protein (chapter 6.1 Figure 3C). As peIF2α is known to induce ATF4 translation we could indirectly assume that GCN2 was not involved in phosphorylation of eIF2α triggered by XRCC1 KD. An involvement of HRI or PKR was not yet studied. However, PKR is known to be activated through double-stranded RNA during viral infection [72] and HRI is predominantly expressed in erythroid cells [73], making it rather unlikely that they played a role in connection to XRCC1 KD.

An interesting auxiliary finding was the strong upregulation of p62 protein in TIG-1 cells upon ATM inhibition alone (Figure 7A and B). Furthermore, direct induction of DNA damage by DNA damaging agents such as H_2O_2 led to a dose dependent reduction of p62 protein (Figure 8). Hence, there was strong evidence that DNA damage signalling was connected to the p62 decrease. In literature we found some report of p62 connected to the DNA-damage response (DDR), for a start there was evidence that p62 could shuttle between cytoplasmic and nuclear compartments, which facilitated its interaction with components of the DNA repair system [74,75]. But the exact mechanism how ATM and DNA damage signalling are connected to p62 will still need to be better investigated.

Besides, we could observe the formation of a second smaller band just above the ordinary p62 band upon ATM inhibition on the Western blot membrane (Figure 7A). This additional band could be appeared due to a post-translational modification such as phosphorylation. There is not much data available in the topic of p62 post-translational modifications. In one study we found phosphorylation of p62 to be able to modulate the nucleocytoplasmic shuttling of p62 [75]. Another group was able to show that p62 phosphorylation was involved in cell cycle regulation in the mitotic phase where phosphorylation was promoted by cdk1 [76]. ATM is known to respond to DNA damage, especially double strand breaks and is an upstream initiator of the checkpoint response, therefore a connection between ATM and cdk1 with following p62 phosphorylation would be feasible [77].

Further investigations in this topic could help to understand other roles of p62 besides its involvement in autophagy. A wider understanding would also help to define possible mechanisms that could provide targets for therapies against CAFs.

7.3.1 The increased survival of XRCC1 KD cells does not depend on upregulation of ASNS promoted by p62 deficiency

Our findings in chapter 6.2.1 suggested that autophagy was unlikely relevant for the increased survival of XRCC1 KD cells under nutrient restriction. For this reason we wanted to investigate other possible mechanisms.

Available data in literature accredited p62 a role in the survival of CAFs under nutrient restriction, specifically under glutamine deprived conditions [42,47]. Low levels of p62 have been found in CAS from prostate and liver cancer, where it promoted CAF-activation [78,79]. In addition to increasing their own survival, p62 deficient CAFs even promoted survival of adjacent tumour cells [47]. As mechanism, a p62 mediated upregulation of ATF4, through enhancing its stability was described [47,48]. This in turn led to enhanced PC expression and upregulation of ASNS which is a known downstream target of ATF4 [49], which led to a metabolic reprogramming enhancing glucose flux into the TCA cycle to facilitate the production of non-essential amino acids, such as Asp and Asn [47]. Because we could display a loss of p62 protein in TIG-1 fibroblasts depleted of XRCC1 we were wondering whether this metabolic reprogramming could also be accountable for the increased survival of XRCC1 KD cells. Knocking-down ASNS together with XRCC1 could not rescue the phenotype of the increased survival under nutrient restriction found in XRCC1 KD cells (Figure 11) even though ASNS was clearly upregulated by XRCC1 KD (Figure 9). This suggests that another mechanism mediates the increased survival of TIG-1 cells depleted of XRCC1.

During the survival assays performed for this project we had the impression that the growth advantage of XRCC1 KD cells differed when FCS lots changed. From literature we knew that FCS composition is quite variable depending for example on seasonal and geographical differences [80,81]. Based on this, we suspected specific components within FCS to be relevant for the survival advantage of XRCC1 KD cells compared to control. Previous research for instance found an upregulation of serine metabolism and an increase in amino acid uptake upon XRCC1 KD [13]. This metabolic shift might alleviate the decrease in other nutrients. Therefore, it would be necessary to define whether the survival advantage of XRCC1 KD cells under nutrient restriction depended on specific components and if so, what exact components play a role. Based on this the future search for the underlying mechanism of XRCC1 KD cells surviving better under nutrient restriction could be more target oriented.

Taken together it would be highly interesting to further investigate the connection of XRCC1 KD and the following loss in p62 protein in CAFs, as there is strong evidence for both to support cancer growth and a better understanding of this connection could provide new starting points for the development of cancer therapies.

7.4 Physiological relevance of XRCC1 downregulation

In addition to the CAF-centred roles of XRCC1 downregulation discussed until now, there also is a potential physiological aspect to it. Under physiological conditions, BER is responsible to maintain genome integrity and prevent accumulation of persistent DNA damage, hence requiring tight coupling of DNA damage levels to BER enzyme levels [15-18]. However, several instances have been described in which BER capacity is specifically lowered in certain cell types under physiological - unstressed - circumstances. Examples for this phenomenon include monocytes, neutrophilic granulocytes, human spermatozoa and terminally differentiated muscle cells [82-85]. It has been suggested that such a BER deficiency could ‘label’ these cells for removal or apoptosis and help the immune system to eliminate these cells [61]. At a closer look, such a mechanism would seem not very logical. As for example monocytes were found among the cells with a physiological BER deficiency, this would mean that all monocytes are collectively targeted for removal by apoptosis or by the immune system as a baseline. Such a mechanism would be quite self-defeating, as monocytes are important players of the immune system, and represent progenitor cells of macrophages and dendritic cells [82,86,87]. While monocytes were shown to lack expression of some essential BER proteins such as XRCC1 and ligase IIIα, in contrast, macrophages and dendritic cells that derive from such monocytes re-expressed these BER proteins and showed normal BER capacity again [88]. This suggests that the transient BER deficiency in monocytes has a special biological function. As one explanation it was speculated that this could provide a regulatory feed-

back loop, where monocytes are killed by ROS-producing macrophages, thereby preventing excessive production of new macrophages that would generate too much ROS in the inflamed tissue [88]. Moreover, also in neutrophilic granulocytes, that derive from the same progenitor cells as monocytes, a decrease of BER capacity was described [84]. Interestingly, in these granulocytes the BER defect seemed to have only a small effect regarding cell death. This was reasoned with the fact that neutrophils anyway just have a lifespan of 1-2 days [89] and it would be detrimental to activate energy-consuming DNA repair processes. In addition, the authors speculated that the BER deficiency could help the cells to undergo apoptosis once they had finished playing their role in defeating infections [84].
Our finding that persistent DNA damage due to a BER deficiency enhances cell survival under stressful conditions such as nutrient restriction could add another, alternative explanation to the phenomenon of a (sometimes transient) physiological BER decrease. Based on our findings, lowering their BER capacity could help these cells to survive under biological challenging conditions, such as in the blood stream for monocytes or in the female reproductive tract for spermatozoa. It would be highly interesting to further pursue this hypothesis.
Taken together, these findings are of relevance and should be further investigated regarding possible side effects of future therapeutic interventions against CAF activation. If a promising target to prevent CAF activation through a BER decline could be found, it should be considered that this intervention could bring disadvantages upon other non-cancer-related cells that lower their BER capacity for physiological reasons.

7.5 Conclusion/Outlook

The first aim of this project was to understand whether downregulation of XRCC1 could enhance cellular survival under nutrient restriction. We could demonstrate a clear survival advantage of XRCC1 KD cells under nutrient restricted growth conditions. It was shown that the KD was consistent in all the conditions, validated by RT-qPCR and Western blot. Furthermore, we were able to show the relevance of ATF4 for the survival advantage of XRCC1 KD cells under nutrient restriction, as a co-knockdown of XRCC1 and ATF4 resulted in a rescue of the observed phenotype in XRCC1 KD cells. These findings are of relevance because understanding the mechanism that lies underneath the increased survival could provide new possibilities for therapeutic intervention to further improve the efficacy of anti-cancer treatments. Therefore, the second aim of the project was to investigate whether activation of autophagy could be a driving force behind such a survival advantage. We demonstrated that there was no significant difference in the autophagic flux of control and XRCC1 KD cells. This suggested that autophagy is likely not relevant for the survival advantage of XRCC1 KD cells under nutrient restriction. As auxiliary interesting finding we detected a loss of p62 protein in cells depleted of XRCC1 that depended on DNA damage signalling through ATM. Further investigations of the connection between p62 decrease and XRCC1 KD could provide a wider understanding of the metabolic changes happening in CAFs especially regarding their survival advantage under nutrient restriction.

8 References

1. World Health Organization. WHO Cancer facts sheet. *www.who.int* Available at: http://www.who.int/en/news-room/fact-sheets/detail/cancer. (Accessed: October 2019)
2. International Agency for Research on Cancer. GLOBOCAN 2020: New Global Cancer Data. Available at: https://www.uicc.org/news/globocan-2020-new-global-cancer-data. (Accessed: 4 February 2021)
3. Valkenburg, K. C., de Groot, A. E. & Pienta, K. J. Targeting the tumour stroma to improve cancer therapy. *Nat Rev Clin Oncol* **15,** 366–381 (2018).
4. Hanahan, D. & Coussens, L. M. Accessories to the Crime: Functionsof Cells Recruited to the Tumor Microenvironment. *Cancer Cell* **21,** 309–322 (2012).
5. Li, H., Fan, X. & Houghton, J. Tumor microenvironment: the role of the tumor stroma in cancer. *J. Cell. Biochem.* **101,** 805–815 (2007).
6. Joyce, J. A. & Pollard, J. W. Microenvironmental regulation of metastasis. *Nat. Rev. Cancer* **9,** 239–252 (2008).
7. Chen, X. & Song, E. Turning foes to friends: targeting cancer-associated fibroblasts. *Nat Rev Drug Discov* 1–17 (2019). doi:10.1038/s41573-018-0004-1
8. Madar, S., Goldstein, I. & Rotter, V. 'Cancer associated fibroblasts'--more than meets the eye. *Trends in Molecular Medicine* **19,** 447–453 (2013).
9. Lindahl, T. Instability and decay of the primary structure of DNA. *Nature* **362,** 709–715 (1993).
10. van Loon, B., Markkanen, E. & Hübscher, U. Oxygen as a friend and enemy: How to combat the mutational potential of 8-oxo-guanine. *DNA Repair (Amst.)* **9,** 604–616 (2010).
11. Markkanen, E. Not breathing is not an option: How to deal with oxidative DNA damage. *DNA Repair (Amst.)* **59,** 82–105 (2017).
12. Dianov, G. L. & Hübscher, U. Mammalian Base Excision Repair: the Forgotten Archangel. *Nucleic Acids Research* (2013). doi:10.1093/nar/gkt076
13. Markkanen, E., Fischer, R., Ledentcova, M., Kessler, B. M. & Dianov, G. L. Cells deficient in base-excision repair reveal cancer hallmarks originating from adjustments to genetic instability. *Nucleic Acids Research* **43,** 3667–3679 (2015).
14. Fan, J. *et al.* XRCC1 down-regulation in human cells leads to DNA-damaging agent hypersensitivity, elevated sister chromatid exchange, and reduced survival of BRCA2 mutant cells. *Environ. Mol. Mutagen.* **48,** 491–500 (2007).
15. Parsons, J. L. *et al.* CHIP-Mediated Degradation and DNA Damage-Dependent Stabilization Regulate Base Excision Repair Proteins. *Mol. Cell* **29,** 477–487 (2008).
16. Parsons, J. L. *et al.* Ubiquitin ligase ARF-BP1/Mule modulates base excision repair. *EMBO J.* **28,** 3207–3215 (2009).
17. Orlando, G., Khoronenkova, S. V., Dianova, I. I., Parsons, J. L. & Dianov, G. L. ARF induction in response to DNA strand breaks is regulated by PARP1. *Nucleic Acids Research* (2013). doi:10.1093/nar/gkt1185
18. Khoronenkova, S. V. & Dianov, G. L. ATM prevents DSB formation by coordinating SSB repair and cell cycle progression. *Proc Natl Acad Sci USA* **112,** 3997–4002 (2015).
19. Tebbs, R. S. *et al.* Requirement for the Xrcc1 DNA base excision repair gene during early mouse development. *Dev. Biol.* **208,** 513–529 (1999).
20. Tebbs, R. S., Thompson, L. H. & Cleaver, J. E. Rescue of Xrcc1 knockout mouse embryo lethality by transgene-complementation. *DNA Repair (Amst.)* **2,** 1405–1417 (2003).
21. Lee, Y. *et al.* The genesis of cerebellar interneurons and the prevention of neural DNA damage require XRCC1. *Nat. Neurosci.* **12,** 973–980 (2009).
22. Hoch, N. C. *et al.* XRCC1 mutation is associated with PARP1 hyperactivation and cerebellar ataxia. *Nature* **541,** 87–91 (2017).
23. Calon, A., Tauriello, D. V. F. & Batlle, E. TGF-beta in CAF-mediated tumor growth and metastasis. *Seminars in Cancer Biology* **25,** 15–22 (2014).

24. Costa, A., Scholer-Dahirel, A. & Mechta-Grigoriou, F. The role of reactive oxygen species and metabolism on cancer cells and their microenvironment. *Seminars in Cancer Biology* **25,** 23–32 (2014).
25. Legrand, A. J. *et al.* Persistent DNA strand breaks induce a CAF-like phenotype in normal fibroblasts. *Oncotarget* **9,** 13666–13681 (2018).
26. Pakos Zebrucka, K. *et al.* The integrated stress response. *EMBO Rep.* **17,** 1374–1395 (2016).
27. Gomes, L., Menck, C. & Leandro, G. Autophagy Roles in the Modulation of DNA Repair Pathways. *Int J Mol Sci* **18,** 2351–21 (2017).
28. Das, G., Shravage, B. V. & Baehrecke, E. H. Regulation and Function of Autophagy during Cell Survival and Cell Death. *Cold Spring Harb Perspect Biol* **4,** a008813–a008813 (2012).
29. Füllgrabe, J., Ghislat, G., Cho, D.-H. & Rubinsztein, D. C. Transcriptional regulation of mammalian autophagy at a glance. *J. Cell. Sci.* **129,** 3059–3066 (2016).
30. He, L. *et al.* Autophagy: The Last Defense against Cellular Nutritional Stress. *Adv Nutr* **9,** 493–504 (2018).
31. Yoshii, S. R. & Mizushima, N. Monitoring and Measuring Autophagy. *Int J Mol Sci* **18,** (2017).
32. Jiang, P. & Mizushima, N. LC3- and p62-based biochemical methods for the analysis of autophagy progression in mammalian cells. *Methods* **75,** 13–18 (2015).
33. B'chir, W. *et al.* The eIF2α/ATF4 pathway is essential for stress-induced autophagy gene expression. *Nucleic Acids Research* **41,** 7683–7699 (2013).
34. Zhang, X. *et al.* Blocking Autophagy in Cancer-Associated Fibroblasts Supports Chemotherapy of Pancreatic Cancer Cells. *Front Oncol* **8,** 590 (2018).
35. Martinez-Outschoorn, U. E. *et al.* Energy transfer in 'parasitic' cancer metabolism. *Cell Cycle* **10,** 4208–4216 (2014).
36. Pavlides, S. *et al.* Warburg Meets Autophagy: Cancer-Associated Fibroblasts Accelerate Tumor Growth and Metastasis viaOxidative Stress, Mitophagy, and Aerobic Glycolysis. *Antioxid. Redox Signal.* **16,** 1264–1284 (2012).
37. Fu, Y. *et al.* The reverse Warburg effect is likely to be an Achilles' heel of cancer that can be exploited for cancer therapy. *Oncotarget* **8,** 57813–57825 (2017).
38. Tanida, I., Ueno, T. & Kominami, E. LC3 and Autophagy. *Methods in Molecular biology (Clifton, N.J.)* **445,** 77–88 (2008).
39. Tanida, I., Minematsu-Ikeguchi, N., Ueno, T. & Kominami, E. Lysosomal turnover, but not a cellular level, of endogenous LC3 is a marker for autophagy. *Autophagy* **1,** 84–91 (2005).
40. Islam, M. A., Sooro, M. A. & Zhang, P. Autophagic Regulation of p62 is Critical for Cancer Therapy. *Int J Mol Sci* **19,** (2018).
41. Bjorkoy, G. *et al. Chapter 12 - Monitoring Autophagic Degradation of p62/SQSTM1*. *Autophagy in Mammalian Systems, Part B* **452,** 181–197 (Elsevier Inc., 2009).
42. Reina-Campos, M., Shelton, P. M., Diaz-Meco, M. T. & Moscat, J. Metabolic reprogramming of the tumor microenvironment by p62 and its partners. *BBA - Reviews on Cancer* **1870,** 88–95 (2018).
43. Katsuragi, Y., Ichimura, Y. & Komatsu, M. p62/SQSTM1 functions as a signaling hub and an autophagy adaptor. *FEBS J.* **282,** 4672–4678 (2015).
44. Moscat, J., Karin, M. & Diaz-Meco, M. T. p62 in Cancer: Signaling Adaptor Beyond Autophagy. *Cell* **167,** 606–609 (2016).
45. Reina-Campos, M., Moscat, J. & Diaz-Meco, M. ScienceDirect Metabolism shapes the tumor microenvironment. *Current Opinion in Cell Biology* **48,** 47–53 (2017).
46. Valencia, T. *et al.* Metabolic reprogramming of stromal fibroblasts through p62-mTORC1 signaling promotes inflammation and tumorigenesis. *Cancer Cell* **26,** 121–135 (2014).

47. Linares, J. F. *et al.* ATF4-Induced Metabolic Reprograming Is a Synthetic Vulnerability of the p62-Deficient Tumor Stroma. *Cell Metab.* **26,** 817–829.e6 (2017).
48. Lassot, I. *et al.* ATF4 Degradation Relies on a Phosphorylation-Dependent Interaction with the SCFβTrCPUbiquitin Ligase. *Molecular and cellular Biology* **21,** 2192–2202 (2001).
49. Fusakio, M. E. *et al.* Transcription factor ATF4 directs basal and stress-induced gene expression in the unfolded protein response and cholesterol metabolism in the liver. *Mol. Biol. Cell* **27,** 1536–1551 (2016).
50. Ahn, C. S. Mitochondria as biosynthetic factories for cancer proliferation. 1–10 (2015). doi:10.1186/s40170-015-0128-2
51. Yoo, H. C., Yu, Y. C., Sung, Y. & Han, J. M. Glutamine reliance in cell metabolism. *Experimental & Molecular Medicine* 1–21 (2020). doi:10.1038/s12276-020-00504-8
52. Jiang, J., Srivastava, S. & Zhang, J. Starve Cancer Cells of Glutamine: Break the Spell or Make a Hungry Monster? *Cancers (Basel)* **11,** (2019).
53. Brem, R. & Hall, J. XRCC1 is required for DNA single-strand break repair in human cells. *Nucleic Acids Research* **33,** 2512–2520 (2005).
54. Nakamura, A. *et al.* Inhibition of GCN2 sensitizes ASNS-low cancer cells to asparaginase by disrupting the amino acid response. *Proc Natl Acad Sci USA* **115,** E7776–E7785 (2018).
55. Zhang, B. *et al.* Asparagine synthetase is an independent predictor of surgical survival and a potential therapeutic target in hepatocellular carcinoma. *Br. J. Cancer* **109,** 14–23 (2013).
56. Wang, L., Cano, M. & Handa, J. T. p62 provides dual cytoprotection against oxidative stress in the retinal pigment epithelium. *Biochim. Biophys. Acta* **1843,** 1248–1258 (2014).
57. Mauthe, M. *et al.* Chloroquine inhibits autophagic flux by decreasing autophagosome-lysosome fusion. *Autophagy* **14,** 1435–1455 (2018).
58. Gottlieb, R. A., Andres, A. M., Sin, J. & Taylor, D. P. J. Untangling autophagy measurements: all fluxed up. *Circ. Res.* **116,** 504–514 (2015).
59. Singleton, D. C. & Harris, A. L. Targeting the ATF4 pathway in cancer therapy. *Expert Opin. Ther. Targets* **16,** 1189–1202 (2012).
60. Rozpedek, W. *et al.* The Role of the PERK/eIF2α/ATF4/CHOP Signaling Pathway in Tumor Progression During Endoplasmic Reticulum Stress. *Curr. Mol. Med.* **16,** 533–544 (2016).
61. Fletcher, S. C. *et al.* Sp1 phosphorylation by ATM downregulates BER and promotes cell elimination in response to persistent DNA damage. *Nucleic Acids Research* **46,** 1834–1846 (2017).
62. Wang, E. Senescent human fibroblasts resist programmed cell death, and failure to suppress bcl2 is involved. *Cancer Res.* **55,** 2284–2292 (1995).
63. Wortel, I. M. N., van der Meer, L. T., Kilberg, M. S. & van Leeuwen, F. N. Surviving Stress: Modulation of ATF4-Mediated Stress Responses in Normal and Malignant Cells. *Trends in Endocrinology & Metabolism* **28,** 794–806 (2017).
64. Boroughs, L. K. & DeBerardinis, R. J. Metabolic pathways promoting cancer cell survival and growth. *Nat. Cell Biol.* 1–9 (2015). doi:10.1038/ncb3124
65. Lyssiotis, C. A. & Kimmelman, A. C. Metabolic Interactions in the Tumor Microenvironment. *Trends Cell Biol.* **27,** 863–875 (2017).
66. Comito, G., Ippolito, L., Chiarugi, P. & Cirri, P. Nutritional Exchanges Within Tumor Microenvironment: Impact for Cancer Aggressiveness. *Front Oncol* **10,** 198–13 (2020).
67. Rzymski, T. *et al.* Regulation of autophagy by ATF4 in response to severe hypoxia. *Oncogene* 1–12 (2019). doi:10.1038/onc.2010.191
68. Mizushima, N. Autophagy: process and function. *Genes Dev.* **21,** 2861–2873 (2007).
69. Kroemer, G., Mariño, G. & Levine, B. Autophagy and the Integrated Stress Response. *Mol. Cell* **40,** 280–293 (2010).

70. Chun, Y. & Kim, J. Autophagy: An Essential Degradation Program for Cellular Homeostasis and Life. *Cells* **7,** 278–26 (2018).
71. Lu, P. D., Harding, H. P. & Ron, D. Translation reinitiation at alternative open reading frames regulates gene expression in an integrated stress response. *Journal of Cell Biology* **167,** 27–33 (2004).
72. Lemaire, P. A., Anderson, E., Lary, J. & Cole, J. L. Mechanism of PKR Activation by dsRNA. *Journal of Molecular Biology* **381,** 351–360 (2008).
73. Han, A. P. *et al.* Heme-regulated eIF2alpha kinase (HRI) is required for translational regulation and survival of erythroid precursors in iron deficiency. *EMBO J.* **20,** 6909–6918 (2001).
74. Hewitt, G. *et al.* SQSTM1/p62 mediates crosstalk between autophagy and the UPS in DNA repair. *Autophagy* **12,** 1917–1930 (2016).
75. Pankiv, S. *et al.* Nucleocytoplasmic Shuttling of p62/SQSTM1 and Its Role in Recruitment of Nuclear Polyubiquitinated Proteins to Promyelocytic Leukemia Bodies. *Journal of Biological Chemistry* **285,** 5941–5953 (2010).
76. Linares, J. F., Amanchy, R., Diaz-Meco, M. T. & Moscat, J. Phosphorylation of p62 by cdk1 Controls the Timely Transit of Cells through Mitosis and Tumor Cell Proliferation. *Molecular and cellular Biology* **31,** 105–117 (2010).
77. Geng, L., Zhang, X., Zheng, S. & Legerski, R. J. Artemis Links ATM to G2/M Checkpoint Recovery via Regulation of Cdk1-Cyclin B. *Molecular and cellular Biology* **27,** 2625–2635 (2007).
78. Duran, A. *et al.* p62/SQSTM1 by Binding to Vitamin D Receptor Inhibits Hepatic Stellate Cell Activity, Fibrosis, and Liver Cancer. *Cancer Cell* **30,** 595–609 (2016).
79. Valencia, T. *et al.* Metabolic reprogramming of stromal fibroblasts through p62-mTORC1 signaling promotes inflammation and tumorigenesis. *Cancer Cell* **26,** 121–135 (2014).
80. van der Valk, J. Fetal bovine serum (FBS): Past – present – future. *ALTEX* 99–118 (2018). doi:10.14573/altex.1705101
81. Baker, M. Reproducibility: Respect Your Cells! *Nature* **537,** 433–435 (2016).
82. Bauer, M. *et al.* Human monocytes are severely impaired in base and DNA double-strand break repair that renders them vulnerable to oxidative stress. *Proc Natl Acad Sci USA* **108,** 21105–21110 (2011).
83. Narciso, L. *et al.* Terminally differentiated muscle cells are defective in base excision DNA repair and hypersensitive to oxygen injury. *Proc. Natl. Acad. Sci. U.S.A.* **104,** 17010–17015 (2007).
84. Ponath, V. *et al.* Compromised DNA Repair and Signalling in Human Granulocytes. *J Innate Immun* **11,** 74–85 (2019).
85. Chan, N. *et al.* Hypoxia Provokes Base Excision Repair Changes and a Repair-Deficient, Mutator Phenotype in Colorectal Cancer Cells. *Molecular Cancer Research* **12,** 1407–1415 (2014).
86. Bauer, M., Goldstein, M., Heylmann, D. & Kaina, B. Human Monocytes Undergo Excessive Apoptosis following Temozolomide Activating the ATM/ATR Pathway While Dendritic Cells and Macrophages Are Resistant. *PLoS ONE* **7,** e39956 (2012).
87. Briegert, M. & Kaina, B. Human monocytes, but not dendritic cells derived from them, are defective in base excision repair and hypersensitive to methylating agents. *Cancer Res.* **67,** 26–31 (2007).
88. Ponath, V. & Kaina, B. Death of Monocytes through Oxidative Burst of Macrophages and Neutrophils: Killing in Trans. *PLoS ONE* **12,** e0170347 (2017).
89. Dancey, J. T., Deubelbeiss, K. A., Harker, L. A. & Finch, C. A. Neutrophil kinetics in man. *J. Clin. Invest.* **58,** 705–715 (1976).

Acknowledgements

Finally, I would like to thank everyone that supported me during my work. Especially as it was not the easiest time with Covid19 present and influencing work and private live.
So, a special thanks goes to the group Markkanen, especially my supervisor Enni Markkanen for giving me the opportunity to elaborate my thesis in her lab and for improvising and leading me through this project despite not being able to be present in person a lot. In addition, I want to thank Zahra Motamed who supported me in some of the experiments as an intern. Furthermore, also a big thank you to Elena Clementi, who did a lot of the work my thesis is based on and for always being reachable when I had questions about her methods or findings.
I would also like to acknowledge the whole Nägeli group and the rest of the Markkanen group for providing a comfortable working area and being helpful in all the small questions that occurred, making the time in the lab very enjoyable and also for being great company in a time where social contacts apart from work were quite limited.
Moreover, I would like to thank the Institute of Veterinary Anatomy and the Center for Clinical Studies for providing some of the equipment used for my work.
Last but not least, I'm very grateful to my family and friends for being patient and supportive in any situation, be it virtual or in person.

Curriculum Vitae

Vorname Name	Larissa Inglin
Geburtsdatum	15.01.1994
Geburtsort	Zug ZG
Nationalität	Schweiz
Heimatort	Sattel SZ

Schulausbildung

08/2000 – 07/2006	Primarschule Rothenthurm, Rothenthurm, Schweiz
08/2007 – 07/2008	Sekundarschule Rothenthurm, Rothenthurm, Schweiz
08/2008 – 07/2012	Kantonsschule Kollegium Schwyz, Schwyz, Schweiz

Höchster Schulabschluss

22/06/2012	Matura, Kantonsschule Kollegium Schwyz, Schwyz, Schweiz

Studium

2013 - 2017	Bachelor of Veterinary Medicine, UZH, Zürich, Schweiz
2017 - 2019	Master of Veterinary Medicine mit Schwerpunkt biomedizinische Forschung, UZH, Zürich, Schweiz

Abschlussprüfung vet. med.

30/12/2019	Universität Zürich, Zürich, Schweiz

Anfertigung der Dissertation

03/2020 - 01/2021	unter der Leitung von PD Dr. med. vet. Dr. sc. nat. Enni Markkanen am Institut für Veterinärpharmakologie und -toxikologie der Vetsuisse-Fakultät Universität Zürich Direktor Prof. Dr. med. vet. Hanspeter Nägeli

03/2020 - 01/2021	Doktorandin, Institut für Veterinärpharmakologie und-toxikologie der Universität Zürich, Zürich, Schweiz